Temporal Regulation of the *Bacillus subtilis* Acetylome and Evidence for a Role of MreB Acetylation in Cell Wall Growth

Valerie J. Carabetta,[a] Todd M. Greco,[b] Andrew W. Tanner,[a] Ileana M. Cristea,[b] David Dubnau[a]

Public Health Research Center at New Jersey Medical School, Rutgers University, Newark, New Jersey, USA[a];
Department of Molecular Biology, Princeton University, Princeton, New Jersey, USA[b]

ABSTRACT N^{ε}-Lysine acetylation has been recognized as a ubiquitous regulatory posttranslational modification that influences a variety of important biological processes in eukaryotic cells. Recently, it has been realized that acetylation is also prevalent in bacteria. Bacteria contain hundreds of acetylated proteins, with functions affecting diverse cellular pathways. Still, little is known about the regulation or biological relevance of nearly all of these modifications. Here we characterize the cellular growth-associated regulation of the *Bacillus subtilis* acetylome. Using acetylation enrichment and quantitative mass spectrometry, we investigate the logarithmic and stationary growth phases, identifying over 2,300 unique acetylation sites on proteins that function in essential cellular pathways. We determine an acetylation motif, EK(ac)(D/Y/E), which resembles the eukaryotic mitochondrial acetylation signature, and a distinct stationary-phase-enriched motif. By comparing the changes in acetylation with protein abundances, we discover a subset of critical acetylation events that are temporally regulated during cell growth. We functionally characterize the stationary-phase-enriched acetylation on the essential shape-determining protein MreB. Using bioinformatics, mutational analysis, and fluorescence microscopy, we define a potential role for the temporal acetylation of MreB in restricting cell wall growth and cell diameter.

IMPORTANCE The past decade highlighted N^{ε}-lysine acetylation as a prevalent posttranslational modification in bacteria. However, knowledge regarding the physiological importance and temporal regulation of acetylation has remained limited. To uncover potential regulatory roles for acetylation, we analyzed how acetylation patterns and abundances change between growth phases in *B. subtilis*. To demonstrate that the identification of cell growth-dependent modifications can point to critical regulatory acetylation events, we further characterized MreB, the cell shape-determining protein. Our findings led us to propose a role for MreB acetylation in controlling cell width by restricting cell wall growth.

KEYWORDS: lysine acetylation, MreB, acetylome, cell wall synthesis, label-free quantification, mass spectrometry, peptidoglycan, posttranslational modification, proteomics

Address correspondence to Ileana M. Cristea, icristea@princeton.edu, or David Dubnau, dubnauda@njms.rutgers.edu.

V.J.C. and T.M.G. contributed equally to this article.

Bacillus subtilis lysine acetylation is temporally regulated throughout growth

The physiological importance of N^{ε}-lysine acetylation as a regulatory posttranslational modification (PTM) is emphasized by the association of its dysregulation with heart disease and aging (1), obesity and diabetes (2), Alzheimer's disease (3), and certain cancers (4). The level of protein acetylation is regulated by the opposing actions of lysine acetyltransferases (KATs) and deacetylases (KDACs). The best understood, evolutionarily conserved family of KATs contains the GCN5-like acetyltransferases

(GNATs), which catalyze the transfer of an acetyl group from acetyl coenzyme A (acetyl-CoA) to a lysine primary amine (5, 6). The deacetylation reaction may be carried out by Zn^+-dependent lysine deacetylases (KDACs) or by NAD^+-dependent sirtuins (7). Acetylation has been shown to affect protein activity (8), protein-protein or protein-DNA interactions (9, 10), local protein conformation (11), and subcellular localization (12, 13).

The advancement of highly accurate and higher-resolution mass spectrometry (MS) techniques combined with the improved specificity of anti-acetyl lysine antibodies has allowed for in-depth, global characterization of cellular acetylomes. Global eukaryotic acetylome studies (14–21) have found that the mitochondrial proteome is highly acetylated, representing nearly 20% of its predicted proteome (21–23). The evolutionary relationship between mitochondria and bacteria has prompted large-scale investigations of acetylation in both Gram-negative (24–35) and Gram-positive (36–43) bacteria. Recently, it has been discovered that acetylation in bacteria is ubiquitous, with hundreds of acetylated proteins potentially affecting many diverse cellular processes.

Despite this growing number of known acetylated proteins in bacteria, the understanding of their function or regulation remains limited. The best-characterized regulatory acetylation in bacteria controls the activity of acetyl-CoA synthetase (AcsA) (31, 44–50). In *Bacillus subtilis*, AcsA is acetylated at a conserved lysine residue within its active site by the KAT enzyme AcuA (51). When increased acetyl-CoA production is required, AcsA is deacetylated by the KDAC homolog AcuC (45) and the sirtuin SrtN (52) and becomes activated. Thus, the activity of AcsA is finely tuned to the levels of acetyl-CoA and NAD^+. Interestingly, this mechanism is evolutionarily conserved, even in human mitochondria (31, 44–50).

Functional roles of other specific acetylation events have not been characterized in *B. subtilis*, which is the best-studied Gram-positive bacterium. Moreover, global analysis of the *B. subtilis* acetylome has thus far been performed at a single time point during stationary-phase growth in rich medium (38) or in media with alternate carbon sources (43). Here, we have characterized the lysine acetylome during both the logarithmic and stationary phases. A quantitative mass spectrometry-based proteomics approach was used to measure temporal changes in protein abundance and acetylation at specific lysine residues. Qualitatively, we have identified acetylation on proteins that cover ~20% of the *B. subtilis* proteome. The identified acetylation sites point to a motif with the core sequence EK(ac)(D/Y/E), in agreement with other bacterial species (24, 27–29, 32, 35, 36, 38, 40, 41, 43) and human mitochondria (14), suggesting conserved regulatory mechanisms. Bioinformatic analysis supports the potential role of acetylation in growth stage-specific regulation of protein function. Based on our differential acetylome analysis, we conducted a functional analysis of the essential cell shape-determining protein MreB, which exhibited a stationary-phase-specific increase in acetylation at a single lysine residue. This characterization suggested a contribution of MreB acetylation in regulating cell wall growth.

RESULTS

Lysine acetylation is prevalent in *B. subtilis* and temporally regulated throughout growth. To characterize the *B. subtilis* acetylome and gain insight into the potential significance of acetylation events, we monitored changes in protein acetylation patterns and abundance. We chose to characterize the dynamic changes occurring during logarithmic (log)- and stationary (stat)-phase growth, because differential acetylation of lysine residues might occur during rapid growth and be of particular relevance for cells progressing from the log into the stat phase. Wild-type cells were grown in minimal glucose medium, and samples were taken for analysis by immunoblotting with anti-acetyllysine antibodies (Fig. 1A, growth curve, indicated by arrows). A striking difference was observed, with prevalent global acetylation during the log phase and a dramatic decrease by the early stat phase (Fig. 1B). To measure changes in lysine acetylation at the level of specific proteins and lysine residues, we designed a mass spectrometry (MS)-based proteomic work flow (Fig. 1A). Isolated acetylated peptides were analyzed

A   Proteomic workflow
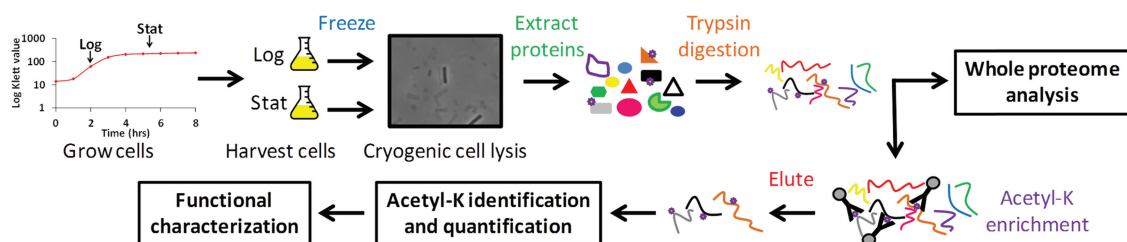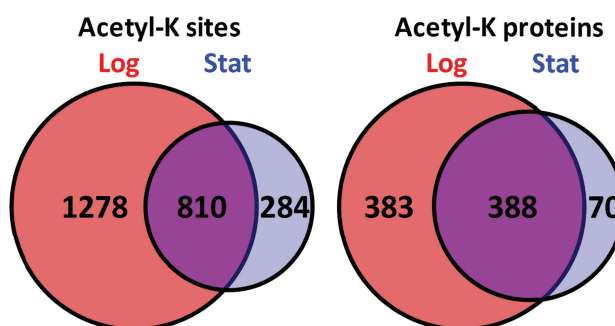

B
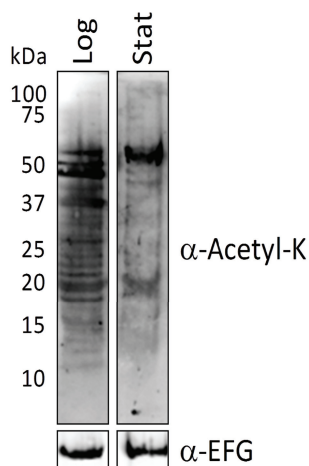
C   Log vs Stat comparisons

FIG 1 Acetylation is a dynamic modification in *B. subtilis*. (A) Wild-type cells (BD630) were grown to the log or stat phase in minimal glucose medium. Arrows on the growth curve indicate the mid-log-phase and early-stat-phase time points used for all studies. Cells were harvested and rapidly frozen for cryogenic cell lysis. This technique was used to obtain a more consistent disruption of the cells, which leads to improved efficiency of protein extraction and reproducibility of acetyl-peptide capture. The image depicts a sample after grinding showing nearly complete cell lysis (>85%). Lysed cell material was resuspended in a heated SDS buffer, and proteins were precipitated and subjected to digestion with trypsin. An aliquot of peptides was saved for whole-cell protein analysis, while the remaining peptides were incubated with agarose beads coated with a mixture of commercially available anti-acetyllysine antibodies. Acetyllysine peptide elutions and peptides from the whole-cell digests were analyzed by label-free quantitative mass spectrometry using nanoscale liquid chromatography (nLC) coupled directly to an LTQ Orbitrap Velos ETD mass spectrometer. Peptide MS/MS sequencing was performed for both sample sets. (B) Wild-type cells were grown to the log and stat phases and lysates prepared as described in Materials and Methods. Equal amounts of protein were loaded in duplicate, with one set probed with a mixture of anti-acetyllysine (acetyl-K) antibodies and the other probed with anti-elongation factor G (anti-EFG) as a loading control. Log- and stat-phase samples were analyzed on the same membrane. (C) Venn diagrams comparing the number of identified acetylated sites (left) and proteins (right) in the log (red) and stat (blue) phases.

by mass spectrometry in three independent biological replicates and two technical replicates. Global proteome changes were also monitored by mass spectrometry at each growth phase to determine whether changes in acetylation corresponded to changes in PTM stoichiometry or overall protein abundance.

We identified 2,372 unique sites on 841 proteins, accounting for ~20% of the predicted proteome (see Table S1 and Fig. S1 in the supplemental material). Of these acetylation sites, 2,088 were detected in the log phase and 1,094 in the stat phase (Fig. 1C). Therefore, mass spectrometry analysis confirmed the global reduction in stat-phase acetylation observed by Western blot analysis of whole-cell lysates (Fig. 1B). As expected, this reduction in the number of sites was accompanied by a reduction in the overall number of acetylated proteins (Fig. 1C; 771 log- and 458 stat-phase proteins). These data demonstrate extensive protein acetylation that is temporally changed depending on growth state. Gene Ontology (GO) analysis (53) of the acetylated proteins showed a significant enrichment of proteins involved in translation, including ribosomal proteins and elongation factors, and enzymes involved in intermediary metabolism (see Fig. S2 in the supplemental material).

Protein properties that influence the presence of acetylation in *B. subtilis*. To further examine the regulation of these acetylation events, we investigated the
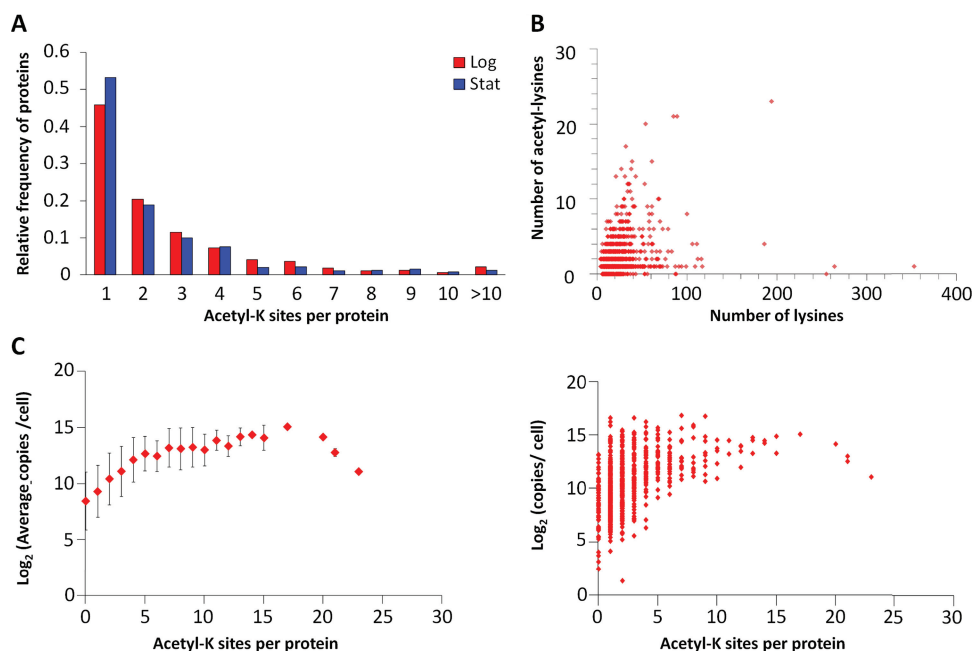
FIG 2 Comparison of the lysine acetylome in the log versus stationary phase. (A) Relative frequency distribution of acetylated proteins normalized to the total number of proteins in each growth phase compared to the number of acetylation sites per protein. (B) Scatter plot showing the distribution of the number of acetylated lysines versus the total number of lysine residues per protein in the log phase. (C) Comparison of acetyllysine sites per protein versus protein copy number estimates for log-phase growth. Protein abundances were expressed as average ± standard deviation (left) or individual (right) values, which were derived from label-free MS analysis.

protein properties that may influence the presence of acetylation. We first assessed the distribution of the number of acetylation sites per protein. Similar patterns were observed for both growth phases (χ^2 test for independence, $P = 0.2369$), with roughly half of the total proteins identified in each phase containing a single acetyllysine modification (Fig. 2A; see Fig. S2B in the supplemental material). The overall number of lysine residues per protein does not appear to influence the distribution of acetylation events for either log- or stat-phase cells, as only a weak correlation was observed between the number of acetylated sites and the total number of lysine residues in each protein (Spearman correlation coefficient [r_s] = 0.1501 and 0.2134, respectively) (Fig. 2B; see Fig. S2C). Thus, the likelihood of identifying an acetylation event is not strictly a function of the number of lysine residues in a given protein, suggesting that there are specific acetylation determinants.

To systematically examine the relationship between protein abundance and the number of identified acetyllysine sites, we used MS1-based quantification of total protein abundance (see Table S2 in the supplemental material) to calculate protein copy numbers (protein molecules per cell). Using this approach, the number of identified acetylation modifications as a function of the average protein abundance clearly showed a positive association for the log ($r_s = 0.5443$) and stat ($r_s = 0.5950$) phases (Fig. 2C, left; see Fig. S2D, top, in the supplemental material). Indeed, we observed that many of the proteins identified with multiple acetylation sites were highly abundant proteins (54). However, the range of protein abundances for defined numbers of acetylation sites was large, particularly for those with a lower number of sites (Fig. 2C, right; see Fig. S2D, bottom). For example, proteins that contained zero or one acetylated lysine spanned the widest abundance range, from <50 copies/cell to >60,000 copies/cell. Conversely, no low-abundance proteins were identified with a large number of acetylated sites (>5 sites) (Fig. 2C, right; see Fig. S2D, bottom). Overall, from these comparisons, there is clearly a protein abundance-dependent component to the identification of the number of acetylated sites, while the number of lysine residues in a protein was less important.
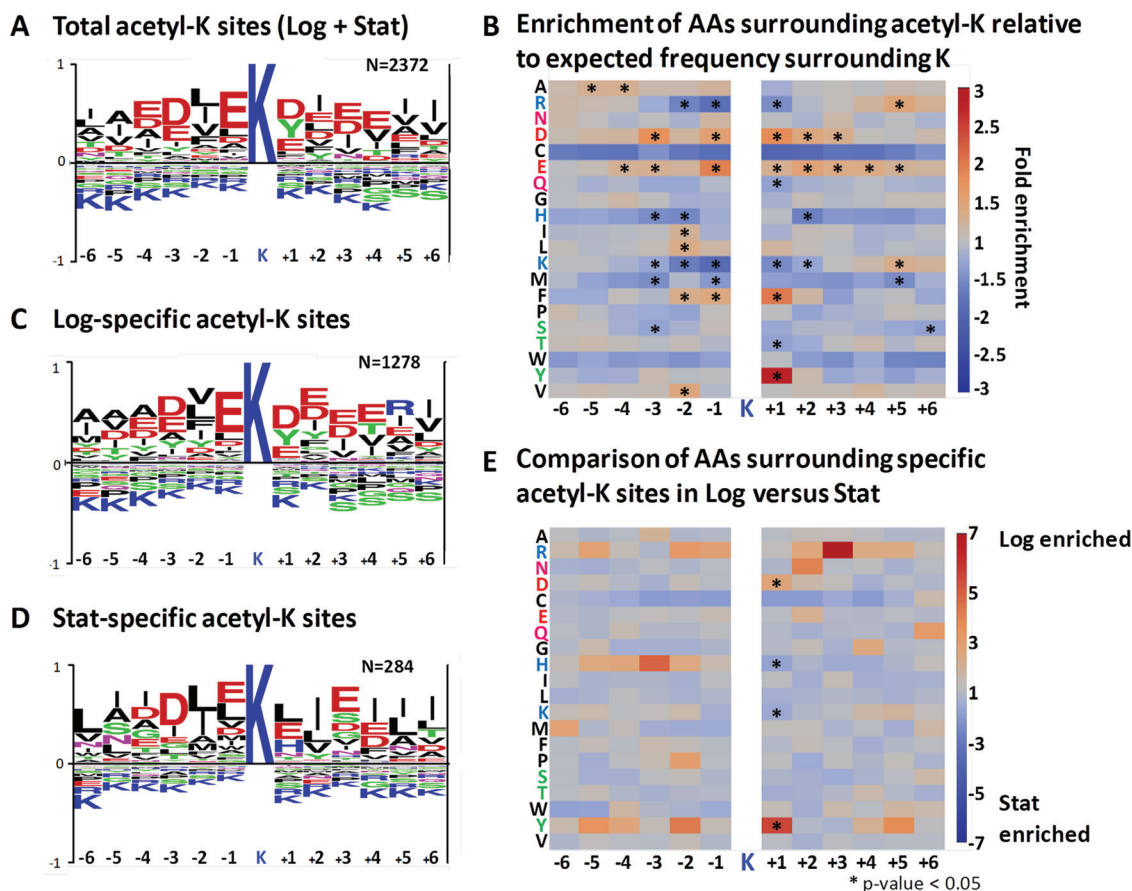
FIG 3 Primary sequence analysis of acetylated protein motifs reveals growth-phase-dependent modification motifs. Sequence windows (±6 residues) surrounding the identified acetylated lysine were analyzed to generate a sequence logo for (A) the entire data set (*n* = 2,372), (C) the log-specific acetylation sites (*n* = 1,278), and (D) the stat-specific (*n* = 284) acetylation sites. (B) Heat map illustrating the fold enrichment of amino acid occurrence for the acetyllysine sequences in panel A relative to the expected amino acid occurrence surrounding all lysine residues in the *B. subtilis* proteome. Statistically significant (Bonferroni corrected *P* values of <0.05) fold enrichment values are indicated by asterisks. (E) Same as panel B, except fold change in amino acid occurrence was compared between log-specific (C) and stat-specific sites (D). The uniform underrepresentation of cysteine did not reach significance because this residue is present at such a low frequency within the *Bacillus* proteome that the differences did not reach significance.

Distinct signature acetylation motifs are present during the log and stat growth phases, pointing to temporal regulation. To investigate the propensity of lysines to undergo acetylation, we examined whether a pattern could be deduced from the primary sequence surrounding the acetylation site. The most prominent sequence motif displayed a preference for acidic residues, accompanied by the underrepresentation of basic residues and the frequent presence of a tyrosine residue at the +1 position (Fig. 3A). The enrichment of acidic residues was significantly overrepresented compared to the overall frequency distribution (Bonferroni-corrected *P* value of <0.05) (Fig. 3B). In addition to acidic residues, tyrosine and phenylalanine were significantly enriched at the +1 position, with tyrosine showing a markedly increased frequency of approximately 3-fold over expectation. Additionally, basic residues (histidine, lysine, and arginine) were significantly underrepresented. These features may represent a recognition sequence for regulatory enzymes, or the local environment may make the target lysine residue a preferred substrate for a nonenzymatic acetylation mechanism (see Discussion).

To determine if acetylation selectivities were different between the log and stat phases, we next analyzed separately the 1,278 and 284 acetylation sites uniquely identified in the log and stat phases, respectively. While the stat-phase-specific set of acetyllysine sites represents a small subpopulation, previous studies have used similar

or smaller numbers to identify possible motifs (24, 27–29, 38–41). Although the log-phase-specific motif closely matched the overall acetylation motif (Fig. 3C versus A), the stat-phase-specific motif slightly diverged from the overall motif (Fig. 3D). Significant differences were found at the +1 position (Fig. 3E): tyrosine and aspartate were strongly favored in the log phase, while basic amino acids, histidine and lysine, were observed in the stat phase (Fig. 3E). In contrast, when the shared log- and stat-phase sites were included, motif analysis yielded results similar to the overall sequence motif (see Fig. S3 in the supplemental material). The identification of a potential acetylation signature for the stat phase points to a possible mechanism for the growth stage regulation of this posttranslational modification.

Signature changes in acetylation during the log- to stat-phase transition include proteins modulating cell structure and morphogenesis. As changes in total protein abundances are primary determinants of cellular function, we next determined the subset of proteins with altered abundances in the stat versus log phase. We identified only 226 proteins that were significantly altered in abundance as cells transitioned from the log to stat phase. DNA-mediated transformation proteins were upregulated, as expected (55), and proteins involved in translation were downregulated (see Fig. S4 and S5 in the supplemental material). Overall, these relatively limited alterations in protein abundance suggest that the identified changes in acetylation are not due to large-scale shifts in proteome composition but rather to the modification stoichiometry.

After establishing the growth phase-dependent changes in total protein, we next evaluated site-specific changes in acetyllysine levels. We found that 271 acetylation sites were significantly downregulated in the stat phase and 92 were upregulated (false discovery rate [FDR], <0.05) (Fig. 4A). The majority of these proteins ($n = 210$) contained a single acetylation site. Interestingly, most of the proteins that contained multiple acetylations ($n = 63$) had sites that were altered in the same direction, meaning that the individual sites were either all up- or downregulated. Yet, one-third of these proteins ($n = 20$) had at least one site that was quantitatively discordant (Fig. 4B). From this subset, the total abundance of all proteins (except SrfAA) remained relatively unchanged from the log to stat phase (see Table S2 in the supplemental material). This implies that the changing acetylation patterns on these particular proteins were not due to increased protein abundance but rather were subject to other regulatory mechanisms. To investigate if the quantitative discordance could be linked to the regulation of protein function; we mapped the differential acetyl sites to known structural features. Indeed, many of these acetylation sites were contained within known functional domains (Fig. 4C; see Fig. S6 in the supplemental material), including nucleotide or substrate binding sites and regulatory domains. While this analysis did not reveal the reason for discordant regulation, the identification of differential acetylation sites within functional domains suggests the possibility that their regulation may be finely tuned by acetyllysine stoichiometry.

We next examined the complete set of differentially acetylated proteins, grouping them by their known enzymatic functions and biological processes. Consistent with previous acetylome studies (19, 24–26, 28, 29, 32, 34–43, 56) and with our qualitative analyses above, differentially acetylated proteins were statistically enriched in metabolic, biosynthetic, and translation processes, largely represented by dehydrogenases, oxidoreductases, ligases, and ribosomal protein functions (Fig. 4D). Only 53% of the proteins were part of the metabolic network, and the remaining set of differentially acetylated proteins were associated with many other areas of bacterial physiology, including transport, DNA metabolic processes, and anatomical structure and morphogenesis (see Fig. S7 in the supplemental material). As these functions have not been linked to acetylation in bacteria, we further analyzed the relationships between the acetylated proteins in these processes. By generating functional and abundance-coded protein networks (Fig. 4E and F), we observed that the majority of the protein expression levels do not significantly change (see Table S2), the lone exception being the single-stranded binding protein SsbA, which increases expression in the stat phase
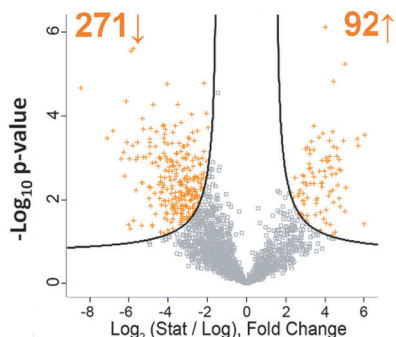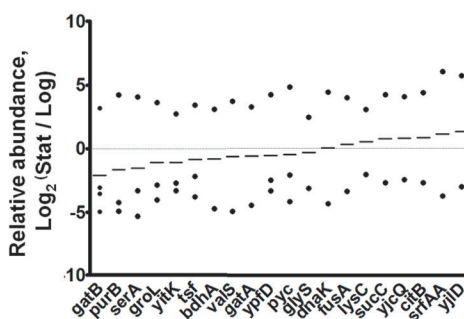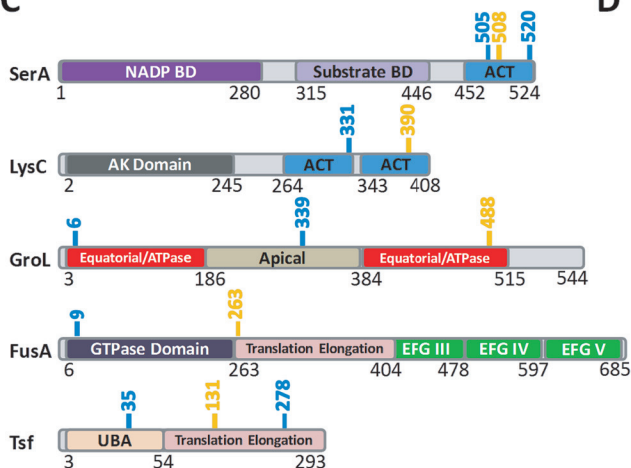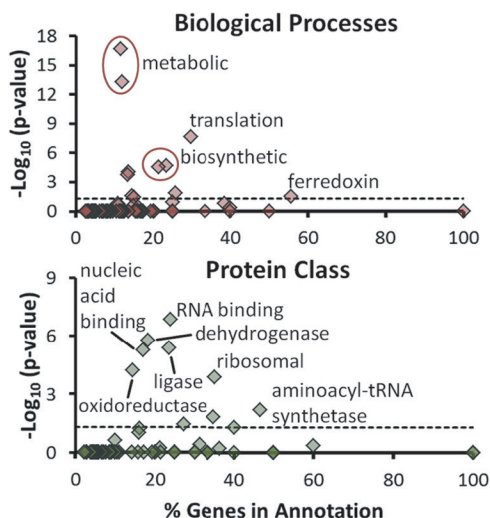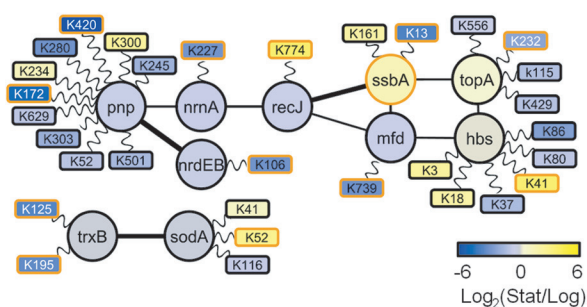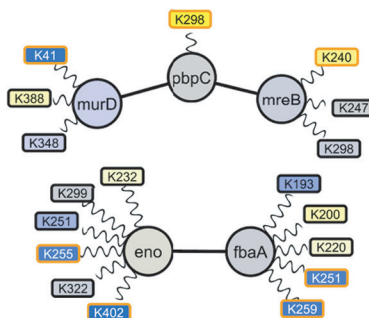
FIG 4 Log- to stationary-phase growth results in differential acetyl abundance on specific proteins. (A) Volcano plot depicting the average site-specific log$_2$ fold change in levels of acetyllysine (n = 1,844 sites). Relative abundances were measured in biological triplicates by MS-based label-free quantification. Acetylation sites with statistically significant differences in abundance (Benjamini-Hochberg FDR, <0.05) are represented by orange crosses. (B) The relative change in acetylation levels of specific acetyllysine sites (filled circles) is shown for the 20 proteins that had at least one discordant site of acetylation. Proteins are sorted by increasing change in the average protein acetylation (horizontal bars). (C) Domain schematics of selected proteins with discordantly regulated acetylation sites. Acetylated residues are denoted by amino acid positions and color coded for downregulated (blue) or upregulated (yellow) relative change in the stat versus log phase. Protein domains were labeled with InterPro terms obtained from UniProtKB. Abbreviations: BD, binding domain; ACT, aspartate kinase, chorismate mutase, and TyrA; AK, aspartate kinase; EFG, elongation factor G; UBA, ubiquitin-associated domain. (D) Gene Ontology annotation and overrepresentation analysis of proteins with differential acetylation. UniProt accession numbers were annotated to PANTHER GO Slim biological processes and protein classes. For each GO term, the percentage of the total annotated genes/proteins that were found differentially acetylated is indicated on the *x* axis. This was compared on the *y* axis to the corresponding statistical significance of overrepresented acetyl proteome gene functions versus the entire genome. The dashed line reflects a Bonferroni-corrected *P* value (P < 0.05). Selected GO terms with the greatest statistical overrepresentation are labeled. (E and F) STRING functional relationships are visualized (solid edges) among the differentially acetylated proteins (circle nodes) in the DNA metabolic process (E) and anatomical structure morphogenesis (F) ClueGO clusters (see Fig. S7 in the supplemental material), along with each protein's corresponding acetylated lysine residue(s) (rectangle nodes). Relative total protein and site-specific acetylation abundance changes are indicated by color scale. Statistically significant abundance changes (see Table S1 in the supplemental material) are indicated by orange node edges.

(Fig. 4E). While we did not determine the absolute stoichiometry of acetylation, by directly measuring both relative protein abundance and relative acetylation abundance, we can make inferences about whether any changes in stoichiometry have occurred. Specifically, we determined that the protein abundances in these networks (Fig. 4E and F) were largely unchanged, while specific acetylations were differentially regulated. Therefore, we concluded that most of the acetylation abundance differences in these networks are bona fide changes in modification stoichiometry.

To our knowledge, acetylation of a structural cytoskeletal protein has not been characterized for prokaryotes. Intriguingly, proteins involved in both the regulation of and the cytoskeleton itself (i.e., actin, and microtubules) are acetylated in eukaryotes (57). In addition, some of these acetylation modifications may have biological significance, such as in the stabilization of actin stress fibers (22) and promotion of the bundling of microtubules (58). MreB, an actin homolog, contains three acetylated residues, 240, 247, and 298; however, only K240 acetylation was significantly increased upon transition to the stat phase (Fig. 4F). In *B. subtilis*, MreB is an essential protein that is primarily responsible for regulating the diameter of the cell (59, 60) and for controlling peptidoglycan (PG) elongation (61–63). Since acetylation is likely to be a regulatory mechanism in controlling the eukaryotic cytoskeleton, we focused on the acetylation of the essential MreB in order to determine its potential regulatory role in cell shape determination in bacteria.

MreB lysine 240 is involved in control of cell width and cell wall biosynthesis. To gain insight into the possible role of MreB K240 acetylation, we first performed a structural analysis. No crystal structure for *B. subtilis* MreB has been determined, so we created a homology model using the *Caulobacter crescentus* structure (PDBe accession no. 4cze [59% sequence identity]). All three lysine residues are predicted to be surface exposed and are clustered to one face of the protein (Fig. 5A). Interestingly, K240 is well conserved in the Gram-positive organisms and is the most conserved of the three acetylation sites (Fig. 5B). The Gram-negative organisms and *Bacillus* paralog Mbl (MreB-like) contain an arginine residue at this position, implying that maintenance of a positive charge is important.

To assess the potential role of acetylation, we constructed glutamine (acetyl-mimic) and arginine (unmodified) single point mutations (64) at the *mreB* native locus. Depletion of MreB was achieved using a strain in which the native copy of *mreB* was deleted and the *mreBCD* genes were placed under inducible control. Since the main function of MreB is in the regulation of cell shape, we determined the length and width of 150 cells in both the log and stat phases. In the log phase, the wild-type cell length averaged 2.88 ± 0.55 μm (Fig. 5C). The K240R and *mreB*-depleted strain cell lengths were nearly identical at 2.75 ± 0.57 μm and 2.81 ± 0.64 μm, respectively. The only statistically significant difference was the length of the K240Q cells, in which the population mean was shorter, with an average of 2.55 ± 0.54 μm ($P < 0.0001$). As wild-type, K240R, and *mreB*-depleted cells enter the stationary phase, they get shorter (1.53 ± 0.28, 1.52 ± 0.29, and 1.52 ± 0.42 μm, respectively) on average (Fig. 5C). Again, the K240Q population was on average even shorter (1.41 ± 0.33 μm; $P = 0.007$). These data indicate that acetylation may have a minor impact on cell length, as the acetyl-mimic MreB showed a modest effect.

We next assessed the impact of acetylation on cell widths (Fig. 5D). Interestingly, the K240Q cells were narrower (0.68 ± 0.09 μm; $P < 0.0001$) than the K240R or wild-type cells (0.75 ± 0.08 and 0.74 ± 0.10 μm, respectively) during the log phase, while the *mreB*-depleted strains were significantly wider (0.97 ± 0.13 μm; $P < 0.0001$), as expected (60, 65). These results suggest that MreB acetylation (K240Q) leads to cell width constriction, as the phenotype is evident during log phase when this residue is not normally acetylated. As wild-type cells enter into stat phase, they become narrower (0.59 ± 0.09 μm). Indeed, the acetylation mimic K240Q (0.56 ± 0.08 μm) was nearly identical to the wild type in cell width. In contrast, both K240R (0.68 ± 0.16 μm; $P < 0.0001$) and *mreB*-depleted (0.74 ± 0.17 μm; $P < 0.0001$) cells were significantly wider. During the stat phase, the observation that the acetyl-mimic mutation (K240Q) did not
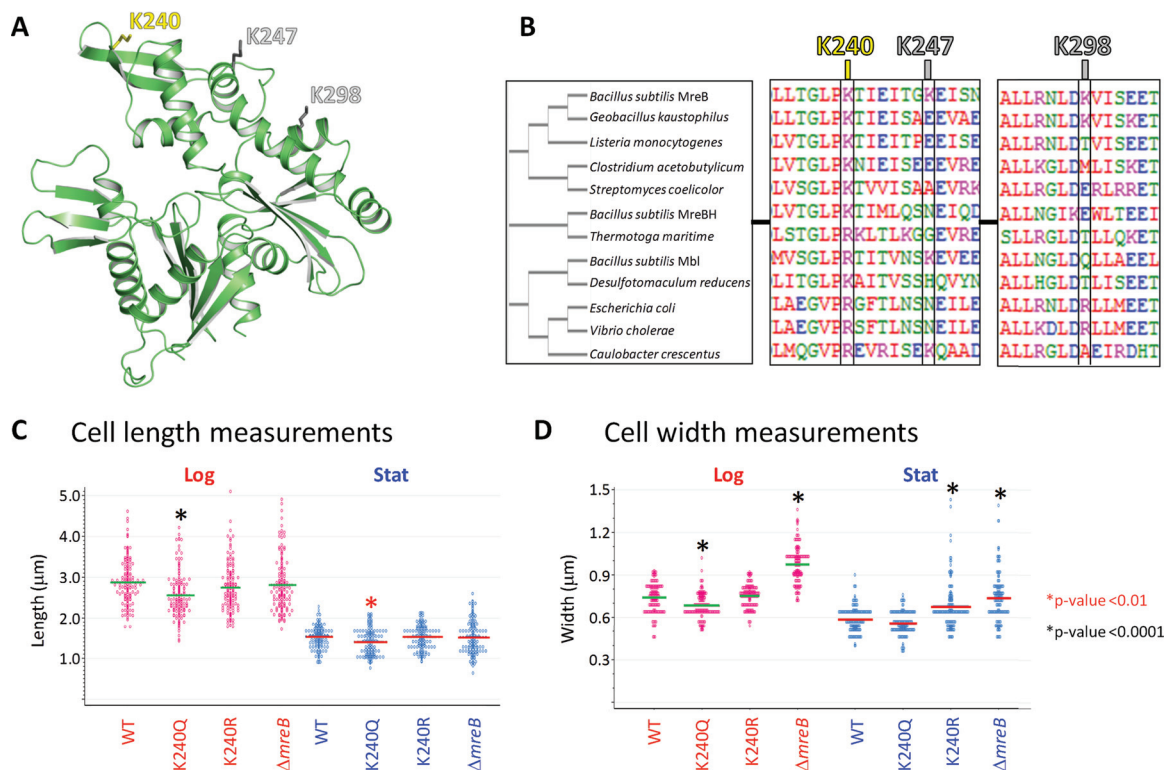
FIG 5 MreB lysine 240 is surface exposed, conserved, and critical for regulating cell size. (A) A ribbon X-ray crystallography model of the *B. subtilis* MreB was generated using the *C. crescentus* structure (PDBe accession no. 4cze; 59% identity) as a template in SWISS-MODEL. The acetylation sites identified in this study are indicated, colored in yellow to indicate an increased abundance in the stat phase, with gray indicating no significant change. (B) ClustalW2 alignment of *B. subtilis* MreB, MreBH, and Mbl with selected bacterial orthologs. The acetylated sites are indicated, color coded as described in panel A. (C and D) Distributional dot plots summarizing *B. subtilis* cell length (C) and width (D) measurements for wild-type (BD630), *mreBK240Q* (BD7587), *mreBK240R* (BD7619), and Δ*mreB* (BD3955) strains (n = 150 cells per strain) grown in the log or stat phase. The middle line (green, log; red, stat) in each plot represents the mean cell length or width. Statistically significant differences in length or width compared to the wild-type strain (Bonferroni-corrected *P* values) are marked with an asterisk.

cause drastic cell width changes while the prevention of acetylation (K240R) led to cell widening is consistent with the fact that K240 was only acetylated during the stat phase. MreB has been implicated in the regulation of PG elongation, so we reasoned that acetylation of K240 may be an important regulatory event in modulating this function. To address this possibility, we stained the cell walls with wheat germ agglutinin (WGA), which binds the PG component *N*-acetylglucosamine. In the log phase, there was a slight reduction in staining in the K240Q mutant, while the K240R mutant appeared to be identical to the wild type (Fig. 6A). However, for the *mreB*-depleted cells, a large increase in WGA staining was evident (Fig. 6A). Upon entry into the stat phase, wild-type cells stain weakly with WGA, and the K240Q mutant stained even less intensely. The K240R cells showed a substantial increase in staining, but not as much as cells with *mreB* depletion (Fig. 6B). These data indicate that the inability to acetylate K240 leads to an alteration of the cell wall, likely affecting the PG. In addition to restricting cell width, the acetylation of lysine 240 may be important for altering cell wall structure as cells enter the stat phase.

DISCUSSION

Determinants of acetylation selectivity and the mechanism of acetylation. We have determined that acetylation site selectivity is dependent upon factors beyond protein abundance (Fig. 2; see Fig. S2 in the supplemental material), most likely neighboring amino acids. Our analysis revealed a statistically significant enrichment for acidic residues in the neighborhood of acetylated lysines and a preference for tyrosine at the +1 position (Fig. 3B). Although it is possible that the identified sequence motifs
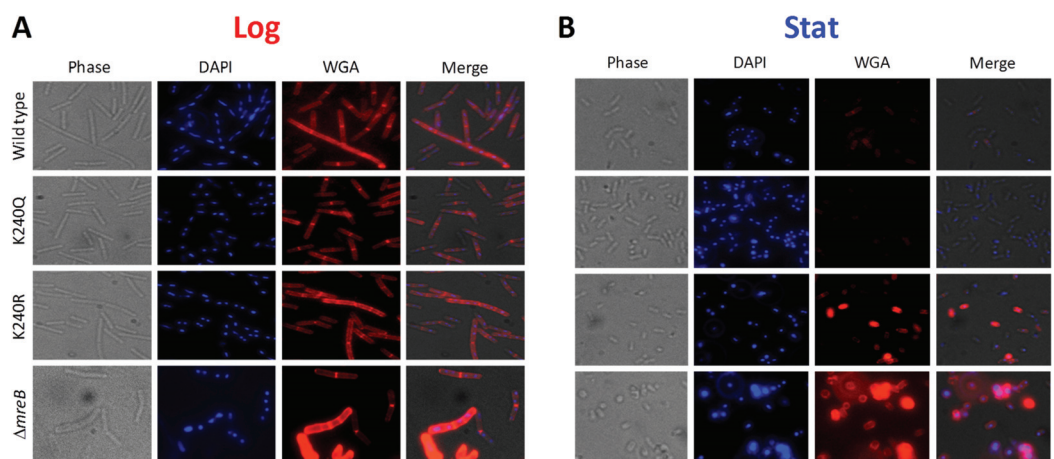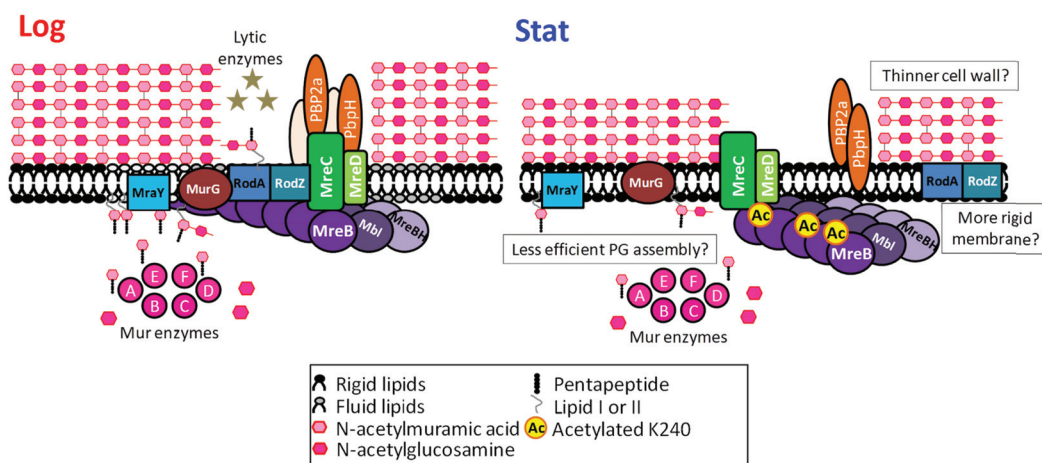
FIG 6 Acetylation mutants alter the peptidoglycan layer of the cell wall. (A and B) Phase-contrast and fluorescence microscopy of wild-type (BD630), *mreBK240Q* (BD7587), *mreBK240R* (BD7619), and *mreB*-depleted (BD3955) cells in the log (A) or stat (B) phase. Depicted are representative images from 2 independent experiments. Cell morphology was visualized by phase contrast, while cell surface saccharides were visualized by wheat germ agglutinin (WGA [red]). DNA was visualized by DAPI (blue). All exposure times were identical for WGA staining, except for the *mreB*-depleted log-phase images, where the exposure time was reduced 5-fold. (C) A hypothetical model for the role of MreB in coordination of cell wall assembly during log- and stat-phase growth. MreB is associated with its two paralogs (Mbl and MreBH), as well as the inner membrane complex of MreC, MreD, RodA, RodZ, MraY, MurG, and various penicillin-binding proteins (including PBP2a and PbpH, among others). In this model, MreB serves as an organizational scaffold to physically bring together cytoplasmic peptidoglycan (PG) precursor synthesis with extracellular PG assembly, leading to efficient cell wall growth. MreB may also associate with regions of increased membrane fluidity. During the stationary phase, acetylation of K240 increases significantly. As this residue does not lie in the regions required to make MreB filaments, we propose that it lies in an important interaction interface. Disruption of the interactions with any of MreB's known interacting partners could lead to dissociation of the complex and a reduction in rate of PG elongation, formation of a thinner cell wall, and/or a change in membrane rigidity. These possibilities are not mutually exclusive and could lead to the shorter and thinner cells observed in the stationary phase.

only represent a subset of the total population of acetylation sites owing to differences in antibody specificity and affinity, our use of two antiacetyllysine antibodies probably served to decrease this potential bias (66). Our identified acetylation motif is in agreement with other bacterial data (24, 27–29, 32, 35, 36, 38, 40, 41, 43), while differing significantly from eukaryotic nuclear and cytoplasmic acetylation motifs. These tend to be enriched in aromatic and basic residues, while histone motifs are glycine rich (14, 21, 67–70).

In eukaryotic cells, the sequence motifs are thought to represent recognition signatures for the three families of identified KATs (71). In prokaryotes, the only known KATs belong to the GNAT family and specifically acetylate AMP-forming acyl-CoA synthetase enzymes at a conserved active site lysine (44, 72). This acetylation site,

LP(R/K)TX(S/T)GKac(L/I)Q(K/R), does not resemble the motifs identified in this study, suggesting that AcuA in *Bacillus* is not responsible for global acetylation. Moreover, we identified a potential unique stat-phase-specific motif in which Asp and His were under- and overrepresented at position +1, respectively, compared to log-specific motifs (Fig. 3C to E). This motif suggests that there is specificity in the selection of acetylation targets, and it could potentially reflect the sequence specificity of unidentified enzymes that are active in the stat phase. Interestingly, a BLAST search of the *B. subtilis* genome revealed about 50 proteins with homology to the ubiquitous Gcn5 family of acetyl-transferases (5, 6), suggesting that additional, uncharacterized protein acetylases may exist.

On the other hand, it is important to consider that many lysine acetylation events may be nonenzymatic. Emerging evidence has led to the proposal that in mitochondria (73, 74) and bacteria (34, 35, 43), a nonenzymatic mechanism contributes to global protein acetylation. In a basic environment, as in the mitochondrial matrix, lysine residues are relatively deprotonated, potentially serving as efficient nucleophiles for nonenzymatic acetylation. This is reminiscent of the reaction mechanism of the GNAT enzymes, which utilize a general base catalyst to deprotonate the target lysine residue, facilitating nucleophilic attack on the carbonyl carbon of the acetyl group in acetyl-CoA (6, 75). For example, the yeast KAT Gcn5p uses a conserved glutamate residue (E173) to deprotonate the target lysine residue (76). Additionally, a eukaryotic N^{α}-acetyltransferase (Naa50p) depends on a tyrosine or histidine residue to act as a general base catalyst (77), which interestingly, were the other 2 amino acids significantly enriched at the +1 position in our identified motifs (Fig. 3). Unlike the mitochondrial lumen, *B. subtilis* maintains a cytoplasmic pH of ~7.4 (78), suggesting a less favorable environment for a nonenzymatic mechanism than in mitochondria. However, the local chemical environment of a target lysine residue would likely influence its nucleophi-licity and may compensate for this difference. Thus, our identified motif may be an essential part of an autocatalytic mechanism for protein acetylation in *B. subtilis*, *Escherichia coli*, and human mitochondria.

For *E. coli* cells grown in minimal medium supplemented with glucose, global lysine acetylation was dramatically increased in the stat phase compared to the log phase, consistent with the increased levels of the metabolic intermediate acetyl-phosphate in the cell (34). Furthermore, a mutation in the enzyme that breaks down acetyl-phosphate (acetate kinase [encoded by *ackA*]) leads to an increase in the intracellular level of acetyl-phosphate and also increases global acetylation (34, 35, 43). From this work, Kuhn et al. proposed that global acetylation in *E. coli* occurs via a nonenzymatic mechanism, with acetyl-phosphate serving as the acetyl source rather than acetyl-CoA (35). However, this pattern is in stark contrast to our observations in *Bacillus*, which show a dramatic decrease in stat-phase protein acetylation (Fig. 1B and C). Although the reasons for the stat-phase decrease in *B. subtilis* are unknown, they may be due to differences in acetate metabolism and therefore levels of the acetylation donor, whether acetyl-CoA or acetyl-phosphate. We regard the likelihood of a nonenzymatic mechanism as an open question. If the acetylation occupancy were found to be very high at a given site, it would seem that the plausibility of an inherently slow nonen-zymatic mechanism would be diminished.

Roles of acetylation in protein regulation. Although thousands of acetylation sites in several bacterial species have been catalogued, the functional relevance remains unknown for nearly all of these modification sites. Our analysis revealed proteins involved in important cellular pathways that were differentially acetylated in the two growth phases (Fig. 4D; see Fig. S7 in the supplemental material). Two interesting examples that had previously not been linked to regulation by acetylation are the DNA metabolism and the anatomical structure and morphogenesis clusters (Fig. 4E and F). In both cases, the acetylation patterns change, while the levels of the proteins themselves are relatively constant. It is possible that these acetylation events regulate protein function, as they often are located within or near known functional

domains. For example, polynucleotide phosphorylase (Pnp) has two sites (K172 and K420) acetylated in the log phase that are predicted to be within exoribonuclease phosphorolytic domains 1 and 2, respectively. Another example is thioredoxin reductase (TrxB), which is acetylated during the log phase at two sites—one (K125) located 10 residues away from the active site and another (K195) within the NAD-binding domain.

An interesting subset of proteins had at least one site that was quantitatively discordant (Fig. 4B), going up or down in the stat phase while other acetylations in the same protein changed in the opposite direction. These discordant patterns hint at specificity in the rates of acetyllysine formation at different sites. If these rates are determined by nonenzymatic mechanisms, then they must be differentially affected by factors that change as cells move into the stat phase (e.g., protein folding or protein-protein interactions). Altogether, the diversity of functional networks that contain specific acetylation sites changing in abundance provides evidence for global regulatory mechanisms acting on different pathways.

Does MreB acetylation regulate cell shape? The phenotypes of the MreB-K240Q and -K240R substitution mutants are consistent with the idea that acetylation of this residue reduces the rate of PG synthesis. The K240Q cells are shorter and narrower in the log phase, show no phenotype in the stat phase, and stain more weakly with WGA, consistent with the exclusive detection of K240 acetylation in the stat phase (Fig. 4F, 5C and D, and 6A and B). Possibly, acetylation leads to a reduction in PG synthesis and a reduction in cell size. In the stat phase, the K240R cells are wider than normal, perhaps due to an inability to acetylate this residue (Fig. 5D). All of the identified MreB acetylation sites, including K240, lie in a surface-exposed region (Fig. 5A) that is not involved in the creation of an interface for interaction with other MreB molecules in the filament (79). Since MreB is believed to be a scaffold protein, this surface may be involved in interaction with other proteins or lipids. Indeed, MreB is known to interact with a number of proteins (Fig. 6C) that are essential for PG elongation, including both cytoplasmic and extracellular components of PG precursor synthesis and assembly (60, 62, 63, 65, 80–84). One proposed role for MreB is to coordinate PG elongation by guiding precursors from the cytoplasm to assembly sites on the surface of the cell (61, 62, 84). It was also recently discovered that MreB filaments are associated with lipid regions of increased fluidity, and MreB itself may be involved in the distribution of lipids and membrane proteins (63). In addition, the PG precursor lipid II has a strong preference for association with fluid membranes (85), which may represent a mechanism by which MreB organizes PG elongation. It is plausible that acetylation of K240 on a population of MreB molecules could disrupt or create new critical contacts made with any of these interacting partners that alter the rate of PG elongation, or some other property of the cell wall (thickness, composition, or membrane rigidity), in the stationary phase to restrict cell size. Taken together, the surface-exposed location of this residue and the observed phenotypes of K240 mutations suggest that this region of the protein may be involved in protein-protein or protein-lipid interactions and that acetylation may modulate these interactions. Although the importance of lysine acetylation is frequently studied using single point mutant substitutions of lysine to either glutamine, regarded as an acetyl-mimic, or arginine, which cannot be acetylated but retains a positive charge (64), caution is essential when interpreting the phenotypic consequences of these substitutions because the side chains of glutamine, acetyllysine, lysine, and arginine are chemically distinct. Nevertheless, this type of analysis has proven useful previously, as glutamine substitutions have been demonstrated to recapitulate the effects of acetylation *in vitro* (86, 87) and *in vivo* (87–90), although not for all proteins (91, 92).

In summary, our study demonstrates that acetylation is prevalent and regulated in *Bacillus subtilis* during the transition from the log phase to the stat phase. Acetylated proteins function in pathways that extend beyond the previously reported translation and central metabolism processes. Our finding that MreB is dynamically modified by

TABLE 1 Strains used in this study

Strain	Relevant genotype	Source[a]
B. subtilis		
BD630	*his leu8 metB5*	Lab strain
BD3955	*his leu8 metB5 amyE::P$_{xyl}$-mreBCD* Spc Δ*mreB*::Kan	This study
BD7587	*his leu8 metB5 mreB-K240Q*	This study
BD7619	*his leu8 metB5 mreB-K240R*	This study
E. coli		
ED1881	Stellar/pminimad2-*mreBCD* Amp	This study
ED1888	Stellar/pminimad2-*mreBCD-K240R* Amp	This study
ED1895	Stellar/pminimad2-*mreBCD-K240Q* Amp	This study

[a]The P$_{xyl}$-*mreBCD* and Δ*mreB*::Kan constructs were kindly provided by R. Daniels and J. Errington.

acetylation during cell growth in a way correlating with cell size suggests a plausible role for regulation by acetylation.

MATERIALS AND METHODS

Bacterial strains, media, and growth conditions. The *Bacillus subtilis* strains used in this study are listed in Table 1. *Bacillus* strains were constructed by transformation with selection for appropriate antibiotics (93). Minimal glucose medium was supplemented with 50 μg/ml histidine, leucine, and methionine. Antibiotics were added where appropriate, and the concentrations used were as follows: 5 μg/ml erythromycin (Ery), 100 μg/ml spectinomycin (Spc), and 5 μg/ml kanamycin (Kan). Bacteria were grown in Luria broth (LB) or minimal medium at 37°C with aeration, and growth was monitored in a Klett colorimeter. Stellar competent cells (Clontech) were used for cloning. Plasmids in *E. coli* were selected for and maintained in the presence of 100 μg/ml ampicillin (Amp).

Plasmid and strain construction. To construct the *mreB* point mutations at the native locus, we utilized the pminimad2 cloning strategy, as described previously (94). The *mreBCD* operon was amplified from BD630 genomic DNA using the primers 5pMM-mreB (5′-<u>TGATTACGCCAAGCTT</u>TGCTAGAGACCTTG GTATAGATCT [in which the underlined portion represents homology to the vector]) and 3pMM-mreD (5′-<u>GTGAATTCGAGCTCGGTACC</u>TCTTCACAATATTCACCTCAAC) and cloned into the HindIII and KpnI sites on plasmid pminimad2 using the In-Fusion HD cloning kit (Clontech), as per the manufacturer's instructions. All oligonucleotides were provided by Eton Biosciences (Union, NJ). The plasmid pminimad2-*mreBCD* (pED1881) was used as a template to create the K240 variants. The plasmid was mutagenized using the Change-IT multiple mutation site-directed mutagenesis kit (Affymetrix), per the manufacturer's instructions, using the primer 5mreBK240Q (5′-CTCACAGGTTTGCCGC<u>C</u>AAACAATTGAAAT TACA [with the mutagenized nucleotide underlined]) or 5mreBK240R (5′-CTCACAGGTTTGCCGA<u>G</u>AACA ATTGAAATTACA). All plasmid constructs were confirmed by sequencing performed by Eton Biosciences. The resulting plasmids, pED1888 and pED1895, were used to transform BD630 to create the *mreB-K240R* (BD7587) and *mreB-K240Q* (BD7619) point mutations at the native locus, respectively. The resulting *Bacillus* strains were confirmed by sequencing.

Western blotting. A 50-ml culture of BD630 was grown in minimal glucose medium until the mid-log phase and stat phase, and 25 ml was pelleted at each time point. Extracts were prepared by resuspending the pellets in 1 ml STM (50 mM Tris-HCl, pH 8.5, 50 mM NaCl, 25% sucrose, 5 mM MgCl$_2$), and the cells were lysed by sonication. Cellular debris was pelleted, and the protein concentration was determined from the resulting supernatants by Bradford assay (BioRad). Samples were mixed with cracking buffer (0.225 M Tris-HCl, pH 6.8, 50% glycerol, 5% sodium dodecyl sulfate [SDS], 0.05% bromophenol blue, 1% β-mercaptoethanol) and boiled for 10 min, and equal amounts of protein were loaded on a 12% Tris-Tricine gel. Proteins were then transferred to a Protran nitrocellulose membrane (Whatman), blocked in 5% bovine serum albumin (BSA), and probed using a mixture of a 1:1,000 dilution of 2 different anti-acetyllysine antibodies (PTM Biolabs and ImmuneChem) in 5% BSA, as per the manufacturer's recommendation. A 1:5,000 dilution of purified goat anti-rabbit antibodies conjugated to peroxidase (Abcam) was used as a secondary antibody. Bands were visualized using the enhanced chemiluminescence ECL Prime kit (Amersham) and imaged using a MyECL imager (Thermo Scientific).

Preparation of cells and cryogenic cell lysis. BD630 was grown overnight at 30°C on multiple glucose minimal medium plates. Cells were scraped from plates, pooled, and used to inoculate 8 liters of liquid glucose minimal medium. Six liters of cells was grown at 37°C to mid-log phase in glucose minimal media or 2 liters was grown to the early stat phase. Cells were harvested, frozen as pellets in liquid nitrogen, and subjected to cryogenic cell lysis as described previously (95–97).

Protein precipitation and trypsin digestion. From the ground frozen cell powder, 0.1 g (previously estimated to be ~3 to 5 mg of protein) was resuspended in 2 ml of TEST buffer {100 mM Tris, pH 8.0, 2% SDS, 5 mM tris(2-carboxyethyl) phosphine [TCEP], 1 mM EDTA} that was previously heated to 95°C. Samples were sonicated and then centrifuged at 21,000 × g for 10 min at 20°C, and the resulting supernatants were heated to 70°C for 10 min for sample reduction. Proteins were alkylated by treatment with 10 mM chloroacetamide (final concentration) for 1 h at 37°C. The reaction was quenched by addition of 10 mM cysteine for 15 min at 37°C. After incubation, samples were cooled on ice, and 4 volumes of ice-cold acetone was slowly added, drop by drop. Tubes were incubated at −20°C for 1 h, and lysates were clarified by centrifugation at 3,000 × g for 10 min at 4°C. The resulting pellets were washed 3 times

with 80% cold acetone and allowed to air dry. The dried pellets were resuspended in a 1-ml solution of 50 mM ammonium bicarbonate, 0.1% RapiGest surfactant (Waters), and 1 mM $CaCl_2$. The protein concentration was determined using a Coomassie (Bradford) protein assay kit (Pierce), and input material was normalized. Precipitated proteins were digested with 50 μg of sequencing-grade modified trypsin (Promega) for 4 h at 37°C, and then a second 50 μg of trypsin was added, and the mixture was allowed to digest overnight. Trypsin was then inactivated by incubation for 5 min at 95°C.

Enrichment of acetylated peptides. The enrichment of acetylated peptides was carried out as described previously, with some modifications (98). The samples were acidified by addition of 1% (final concentration) trifluoroacetic acid (TFA) and incubated for 45 min at 37°C to cleave the RapiGest. The peptide solutions were centrifuged at 21,000 × g for 10 min at 20°C, and the pellets were discarded. The supernatants were split equally into 4 tubes, dried to completeness by vacuum centrifugation, and then each washed with 1 ml high-performance liquid chromatography (HPLC)-grade water and dried to completeness. This was repeated 3 times until no visible salt pellet remained. The lyophilized pellets were resuspended and combined in a total volume of 1.5 ml NETNA binding buffer (50 mM Tris-HCl, pH 8.0, 100 mM NaCl, 1 mM EDTA, 0.5% NP-40, 10% acetonitrile [ACN]). Centrifugation was performed at 21,000 × g for 10 min to remove any remaining insoluble material. From the supernatants, aliquots of ~50 μg of peptides were reserved for total cell protein analysis, and then a mixture of 50 μl of prepared pan acetyllysine antibody (PTM Biolabs) conjugated to protein A beads (Santa Cruz Biotechnology) and 50 μl of a commercial anti-acetyllysine antibody agarose (ImmuneChem) was added and allowed to incubate for 5 h at 4°C with rotary shaking. Conjugation of antiacetyllysine antibody to protein A agarose beads was carried out as described previously (98). The beads were collected by centrifugation at 1000 × g for 2 min and then washed 3 times with 1 ml of NETN buffer (50 mM Tris-HCl, pH 8.0, 100 mM NaCl, 1 mM EDTA, 0.5% NP-40), 3 times with ETN (50 mM Tris-HCl, pH 8.0, 100 mM NaCl, 1 mM EDTA), and finally 1 time with 1 ml HPLC water at 1,000 × g for 2 min at 4°C for each wash. Peptides were eluted from the beads with 150 μl of elution buffer (0.5% TFA, 5% ACN), repeated 3 times. Our enrichment efficiency was routinely between 25 and 40%. The pooled supernatants from acetyllysine enrichment were concentrated by vacuum centrifugation. Both acetyllysine supernatants and total cell digests were acidified to 1% TFA. SDB-RPS (Empore [3 M]) StageTips were used to desalt samples, and for total cell digests, peptides were separated by stepwise elution into three fractions, as previously described (99). The lysine enrichment and whole-cell digest analyses were repeated 3 independent times.

Mass spectrometry analysis of acetyllysine enrichments and whole-cell digests. Peptides (4 μl) from biological triplicates of acetyllysine peptide enrichments and corresponding whole-cell lysate digests from the log and stat phases were analyzed by nanoscale liquid chromatography (nLC) coupled online to either an LTQ Orbitrap Velos (acetyllysine) or XL (whole-cell) mass spectrometer (Thermo Fisher Scientific, Inc.). Peptides were loaded directly on column (PepMap C_{18} RSLC: 1.8 μm, 75 μm by 50 cm) and resolved by reverse-phase chromatography using a linear 3-h gradient of 4 to 40% buffer B (A, 0.1% formic acid in H_2O; B, 97% ACN in 0.1% formic acid). Eluted peptides were analyzed by data-dependent acquisition (DDA) methods. Briefly, full MS spectra were acquired in the Orbitrap analyzer (resolution, 30,000; lock mass enabled for the Velos), from which precursors were selected for tandem MS (MS/MS) fragmentation. To increase the coverage and confidence of the identified acetylations, the complementary fragmentation techniques, collision-induced dissociation (CID [Top 15]) and higher-energy C-trap dissociation (HCD [Top 10]) were employed in two separate technical replicate DDA runs. HCD fragmentation provided signature immonium ion fragments diagnostic for acetyllysine. For whole-cell analysis, DDA CID (Top 10) fragmentation was employed. In all runs, the following instrument settings were used: Fourier transform MS (FTMS) and ion trap MS (ITMS) target values of 1E6 and 1E4 (Velos) or 5E3 (XL), respectively, and FTMS and ITMS maximum ion times of 500 and 100 ms, respectively. Dynamic exclusion was enabled with a repeat count of 1.

Peptide identification and label-free protein quantification. Thermo RAW instrument files for both acetyllysine enrichment and whole-cell data sets were processed together using MaxQuant (version 1.5.2.8) for peptide identification and label-free quantification. For the MaxQuant experimental design, the acetyllysine and whole-cell data sets were defined as separate parameter groups. MS/MS spectra were extracted using the default settings, and the database search was performed against the UniProt SwissProt/TrEMBL *Bacillus subtilis* (strain 168) sequence database (release 2015-02, 4,243 sequences), appended with common contaminants. The search parameters were configured identically for each parameter group, allowing for variable modification of oxidized methionine and protein N-terminal and lysine acetylation, as well as fixed modification of cysteine carbamidomethylation. Transferring of MS/MS sequencing events to nonsequenced features in other runs was enabled. However, to maintain the protein-level quantitative accuracy of the whole-cell data set, the label-free quantification (LFQ) algorithm (100), which employs mass recalibration and between-run peptide-level normalization, was performed separately within each parameter group. In addition, acetyllysine-containing peptides were excluded from protein quantification. To control false identification rates, PSM, protein, and site FDR were set at 1%, calculated based on matches to a reverse database. MaxQuant result files were imported into Perseus (version 1.5.1.6) for quantitative analysis, specifically acetyllysine peptides with their corresponding peptide intensity values, and protein groups with their corresponding LFQ abundance values (whole cell). Acetyllysine peptides were filtered to require (i) at least two valid intensity values in at least one group and (ii) a minimum PTM localization probability of 0.75. For whole-cell analyses, protein group assignments were filtered to require (i) at least two valid intensity values in at least one group and (ii) at least two sequenced razor + unique peptide identifications. After filtering, missing values were addressed by imputation based on a normal distribution using default settings. Differentially regulated acetyllysine sites and cellular proteins were determined using the Volcano plot function ($S_0 = 1$; FDR,

<0.05), computing FDR-corrected *P* values (*t* test) versus the magnitude of fold change (stat/log phase). Protein copy numbers were estimated based on 0.25 pg of protein per cell and using LFQ values normalized by the theoretical number of tryptic peptides (101). Processed and filtered data were exported to Microsoft Excel for further bioinformatics analysis.

Bioinformatics and functional pathway analysis. For GO analysis, primary accession numbers of proteins identified from whole-cell or acetyllysine peptide capture experiments were submitted to the Panther GO databases (www.pantherdb.org) or the ClueGO cytoscape plug-in (version 2.1.6) (102). The Panther GO analysis was used for statistical overrepresentation of individual biological processes, while ClueGO was used to generate biological process networks using ontology clustering. ClueGO was used to compare the biological processes shared between two lists of accession numbers and to generate GO biological process networks (both with grouping enabled, kappa score = 0.4). UniProt accession numbers were submitted to STRING (version 10) (103) to generate protein-protein functional networks. STRING networks were imported into cytoscape (version 3.2.1) (104) for overlay of quantitative data. All acetyllysine sites and neighboring amino acids were analyzed by the PhosphoSite motif and logo analysis tool (105). The *Caulobacter crescentus* (4cze.1.A, 59% identity) MreB structure was used as a template to create a homology model using SWISS-MODEL software (106). ClustalW2 (107) was used to generate the cladogram and sequence alignment.

Statistical analysis. Calculations of differences between actual versus expected lysine frequency were performed utilizing a comparison of proportions and applying a Bonferroni correction to *P* values for multiple comparisons (108) using Microsoft Excel 2010. The test of independence comparing log- and stat-phase acetyllysine distributions was performed similarly. All subsequent statistical analyses were performed using Stata/SE 13.1. While the utilization of Pearson's correlation coefficient is more common when analyzing the correlation between variables, we wanted to look at a more general association between lysine number or protein abundance and number of acetylation sites. For this reason we used a Spearman rank correlation, since it is not limited to simple linear relationships and is also nonparametric (109). The distributional dot plots were constructed using Stata/SE 13.1. Differences between mean width and length were analyzed using a one-way analysis of variance (ANOVA) followed by *post hoc t* test. All *P* values displayed have been Bonferroni corrected to account for multiple comparisons.

Microscopy. *Bacillus* strains were grown in LB medium to the mid-log or stat phase. For cell length measurements, at each time point 500 µl of cells was harvested, and the cells were incubated for 5 min in 2 µg/ml propidium iodide (PI) on poly-L-lysine-coated slides, washed 10× with phosphate-buffered saline (PBS; 81 mM Na_2HPO_4 plus 24.6 mM NaH_2PO_4 plus 100 mM NaCl), and then mounted in Slowfade (Molecular Probes). For wheat germ agglutinin (WGA [Life Technologies]) staining, cells were attached to a poly-L-lysine-coated slide, incubated for 1 min in the presence of 2 mg/ml (final concentration) lysozyme, and then immediately washed three times in PBS. Cells were stained for 15 min with 2 µg/ml (final concentration) 4′,6-diamidino-2-phenylindole (DAPI) and 1 µg/ml WGA and then washed and mounted as described above. Microscopy was performed with an upright Nikon Eclipse 90i microscope outfitted with an Orca-ER digital camera (Hamamatsu) and a Nikon TIRF 1.45 NA Plan Neo-Fluor 100× oil immersion objective. The Volocity software package (version 6.3; PerkinElmer) was used for image acquisition and measurements. The exposure time for the WGA staining was 50 ms for every strain in both growth phases, with the exception of the *mreB* mutant in log phase, which was imaged for 10 ms. For individual cell measurements, the length and width of 150 cells were determined for each strain.

SUPPLEMENTAL MATERIAL

Supplemental material for this article may be found at http://dx.doi.org/10.1128/mSystems.00005-16.

Figure S1, EPS file, 1.4 MB.
Figure S2, EPS file, 2.6 MB.
Figure S3, PDF file, 2.5 MB.
Figure S4, PDF file, 2.6 MB.
Figure S5, PDF file, 2.8 MB.
Figure S6, PDF file, 1 MB.
Figure S7, PDF file, 0.2 MB.
Table S1, XLSX file, 0.6 MB.
Table S2, XLSX file, 1 MB.

REFERENCES

1. **Wagner GR, Payne RM**. 2011. Mitochondrial acetylation and diseases of aging. J Aging Res **2011:**234875. http://dx.doi.org/10.4061/2011/234875.

2. **Iyer A, Fairlie DP, Brown L**. 2012. Lysine acetylation in obesity, diabetes and metabolic disease. Immunol Cell Biol **90:**39–46. http://dx.doi.org/10.1038/icb.2011.99.

3. **Irwin DJ, Cohen TJ, Grossman M, Arnold SE, Xie SX, Lee VM, Trojanowski JQ**. 2012. Acetylated tau, a novel pathological signature in Alzheimer's disease and other tauopathies. Brain **135:**807–818. http://dx.doi.org/10.1093/brain/aws013.

4. **Arif M, Senapati P, Shandilya J, Kundu TK**. 2010. Protein lysine acetylation in cellular function and its role in cancer manifestation. Biochim Biophys Acta **1799:**702–716. http://dx.doi.org/10.1016/j.bbagrm.2010.10.002.

5. **Neuwald A, Landsman D**. 1997. GCN5-related histone N-acetyltransferases belong to a diverse superfamily that includes the yeast SPT10 protein. Trends Biochem Sci **22:**154–155. http://dx.doi.org/10.1016/S0968-0004(97)01034-7.

6. **Dyda F, Klein DC, Hickman AB**. 2000. GCN5-related N-acetyltransferases: a structural overview. Annu Rev Biophys Biomol Struct **29:**81–103. http://dx.doi.org/10.1146/annurev.biophys.29.1.81.

7. **Grozinger CM, Schreiber SL**. 2002. Deacetylase enzymes: biological functions and the use of small-molecule inhibitors. Chem Biol **9:**3–16. http://dx.doi.org/10.1016/S1074-5521(02)00092-3.

8. **Zhang T, Wang S, Lin Y, Xu W, Ye D, Xiong Y, Zhao S, Guan KL**. 2012. Acetylation negatively regulates glycogen phosphorylase by recruiting protein phosphatase 1. Cell Metab **15:**75–87. http://dx.doi.org/10.1016/j.cmet.2011.12.005.

9. **Gu W, Roeder RG**. 1997. Activation of p53 sequence-specific DNA binding by acetylation of the p53 C-terminal domain. Cell **90:**595–606. http://dx.doi.org/10.1016/S0092-8674(00)80521-8.

10. **Glozak MA, Sengupta N, Zhang X, Seto E**. 2005. Acetylation and deacetylation of non-histone proteins. Gene **363:**15–23. http://dx.doi.org/10.1016/j.gene.2005.09.010.

11. **Howe FS, Boubriak I, Sale MJ, Nair A, Clynes D, Grijzenhout A, Murray SC, Woloszczuk R, Mellor J**. 2014. Lysine acetylation controls local protein conformation by influencing proline isomerization. Mol Cell **55:**733–744. http://dx.doi.org/10.1016/j.molcel.2014.07.004.

12. **Li T, Diner BA, Chen J, Cristea IM**. 2012. Acetylation modulates cellular distribution and DNA sensing ability of interferon-inducible protein IFI16. Proc Natl Acad Sci U S A **109:**10558–10563. http://dx.doi.org/10.1073/pnas.1203447109.

13. **Ishfaq M, Maeta K, Maeda S, Natsume T, Ito A, Yoshida M**. 2012. Acetylation regulates subcellular localization of eukaryotic translation initiation factor 5A (eIF5A). FEBS Lett **586:**3236–3241. http://dx.doi.org/10.1016/j.febslet.2012.06.042.

14. **Choudhary C, Kumar C, Gnad F, Nielsen ML, Rehman M, Walther TC, Olsen JV, Mann M**. 2009. Lysine acetylation targets protein complexes and co-regulates major cellular functions. Science **325:**834–840. http://dx.doi.org/10.1126/science.1175371.

15. **Fritz KS, Galligan JJ, Hirschey MD, Verdin E, Petersen DR**. 2012. Mitochondrial acetylome analysis in a mouse model of alcohol-induced liver injury utilizing SIRT3 knockout mice. J Proteome Res **11:**1633–1643. http://dx.doi.org/10.1021/pr2008384.

16. **Henriksen P, Wagner SA, Weinert BT, Sharma S, Bacinskaja G, Rehman M, Juffer AH, Walther TC, Lisby M, Choudhary C**. 2012. Proteome-wide analysis of lysine acetylation suggests its broad regulatory scope in Saccharomyces cerevisiae. Mol Cell Proteomics **11:**1510–1522. http://dx.doi.org/10.1074/mcp.M112.017251.

17. **Kaluarachchi Duffy S, Friesen H, Baryshnikova A, Lambert JP, Chong YT, Figeys D, Andrews B**. 2012. Exploring the yeast acetylome using functional genomics. Cell **149:**936–948. http://dx.doi.org/10.1016/j.cell.2012.02.064.

18. **Weinert BT, Wagner SA, Horn H, Henriksen P, Liu WR, Olsen JV, Jensen LJ, Choudhary C**. 2011. Proteome-wide mapping of the Drosophila acetylome demonstrates a high degree of conservation of lysine acetylation. Sci Signal **4:**ra48. http://dx.doi.org/10.1126/scisignal.2001902.

19. **Wu X, Oh MH, Schwarz EM, Larue CT, Sivaguru M, Imai BS, Yau PM, Ort DR, Huber SC**. 2011. Lysine acetylation is a widespread protein modification for diverse proteins in Arabidopsis. Plant Physiol **155:**1769–1778. http://dx.doi.org/10.1104/pp.110.165852.

20. **Xue B, Jeffers V, Sullivan WJ, Uversky VN**. 2013. Protein intrinsic disorder in the acetylome of intracellular and extracellular Toxoplasma gondii. Mol Biosyst **9:**645–657. http://dx.doi.org/10.1039/c3mb25517d.

21. **Smith KT, Workman JL**. 2009. Introducing the acetylome. Nat Biotechnol **27:**917–919. http://dx.doi.org/10.1038/nbt1009-917.

22. **Kim SC, Sprung R, Chen Y, Xu Y, Ball H, Pei J, Cheng T, Kho Y, Xiao H, Xiao L, Grishin NV, White M, Yang XJ, Zhao Y**. 2006. Substrate and functional diversity of lysine acetylation revealed by a proteomics survey. Mol Cell **23:**607–618. http://dx.doi.org/10.1016/j.molcel.2006.06.026.

23. **Rardin MJ, Newman JC, Held JM, Cusack MP, Sorensen DJ, Li B, Schilling B, Mooney SD, Kahn CR, Verdin E, Gibson BW**. 2013. Label-free quantitative proteomics of the lysine acetylome in mitochondria identifies substrates of SIRT3 in metabolic pathways. Proc Natl Acad Sci U S A **110:**6601–6606. http://dx.doi.org/10.1073/pnas.1302961110.

24. **Zhang J, Sprung R, Pei J, Tan X, Kim S, Zhu H, Liu CF, Grishin NV, Zhao Y**. 2009. Lysine acetylation is a highly abundant and evolutionarily conserved modification in Escherichia coli. Mol Cell Proteomics **8:**215–225. http://dx.doi.org/10.1074/mcp.M800187-MCP200.

25. **Zhang K, Zheng S, Yang JS, Chen Y, Cheng Z**. 2013. Comprehensive profiling of protein lysine acetylation in Escherichia coli. J Proteome Res **12:**844–851. http://dx.doi.org/10.1021/pr300912q.

26. **Wang Q, Zhang Y, Yang C, Xiong H, Lin Y, Yao J, Li H, Xie L, Zhao W, Yao Y, Ning ZB, Zeng R, Xiong Y, Guan KL, Zhao S, Zhao GP**. 2010. Acetylation of metabolic enzymes coordinates carbon source utilization and metabolic flux. Science **327:**1004–1007. http://dx.doi.org/10.1126/science.1179687.

27. **Wu X, Vellaichamy A, Wang D, Zamdborg L, Kelleher NL, Huber SC, Zhao Y**. 2013. Differential lysine acetylation profiles of Erwinia amylovora strains revealed by proteomics. J Proteomics **79:**60–71. http://dx.doi.org/10.1016/j.jprot.2012.12.001.

28. **Okanishi H, Kim K, Masui R, Kuramitsu S**. 2013. Acetylome with structural mapping reveals the significance of lysine acetylation in Thermus thermophilus. J Proteome Res **12:**3952–3968. http://dx.doi.org/10.1021/pr400245k.

29. **Pan J, Ye Z, Cheng Z, Peng X, Wen L, Zhao F**. 2014. Systematic analysis of the lysine acetylome in Vibrio parahemolyticus. J Proteome Res **13:**3294–3302. http://dx.doi.org/10.1021/pr500133t.

30. **Colak G, Xie Z, Zhu AY, Dai L, Lu Z, Zhang Y, Wan X, Chen Y, Cha YH, Lin H, Zhao Y, Tan M**. 2013. Identification of lysine succinylation substrates and the succinylation regulatory enzyme CobB in Escherichia coli. Mol Cell Proteomics **12:**3509–3520. http://dx.doi.org/10.1074/mcp.M113.031567.

31. **Crosby HA, Pelletier DA, Hurst GB, Escalante-Semerena JC**. 2012. System-wide studies of N-lysine acetylation in Rhodopseudomonas palustris reveal substrate specificity of protein acetyltransferases. J Biol Chem **287:**15590–15601. http://dx.doi.org/10.1074/jbc.M112.352104.

32. **Mo R, Yang M, Chen Z, Cheng Z, Yi X, Li C, He C, Xiong Q, Chen H, Wang Q, Ge F**. 2015. Acetylome analysis reveals the involvement of lysine acetylation in photosynthesis and carbon metabolism in the model cyanobacterium Synechocystis sp. PCC 6803. J Proteome Res **14:**1275–1286. http://dx.doi.org/10.1021/pr501275a.

33. **Yu BJ, Kim JA, Moon JH, Ryu SE, Pan JG**. 2008. The diversity of

lysine-acetylated proteins in *Escherichia coli*. J Microbiol Biotechnol **18:**1529–1536.

34. **Weinert BT, Iesmantavicius V, Wagner SA, Schölz C, Gummesson B, Beli P, Nyström T, Choudhary C**. 2013. Acetyl-phosphate is a critical determinant of lysine acetylation in *E. coli*. Mol Cell **51:**265–272. http://dx.doi.org/10.1016/j.molcel.2013.06.003.

35. **Kuhn ML, Zemaitaitis B, Hu LI, Sahu A, Sorensen D, Minasov G, Lima BP, Scholle M, Mrksich M, Anderson WF, Gibson BW, Schilling B, Wolfe AJ**. 2014. Structural, kinetic and proteomic characterization of acetyl phosphate-dependent bacterial protein acetylation. PLoS One **9:**e94816. http://dx.doi.org/10.1371/journal.pone.0094816.

36. **Zhang Y, Wu Z, Wan X, Liu P, Zhang J, Ye Y, Zhao Y, Tan M**. 2014. Comprehensive profiling of lysine acetylome in *Staphylococcus aureus*. Sci China Chem **57:**732–738. http://dx.doi.org/10.1007/s11426-014-5100-4.

37. **Lee DW, Kim D, Lee YJ, Kim JA, Choi JY, Kang S, Pan JG**. 2013. Proteomic analysis of acetylation in thermophilic *Geobacillus kaustophilus*. Proteomics **13:**2278–2282. http://dx.doi.org/10.1002/pmic.201200072.

38. **Kim D, Yu BJ, Kim JA, Lee YJ, Choi SG, Kang S, Pan JG**. 2013. The acetylproteome of Gram-positive model bacterium *Bacillus subtilis*. Proteomics **13:**1726–1736. http://dx.doi.org/10.1002/pmic.201200001.

39. **Liu F, Yang M, Wang X, Yang S, Gu J, Zhou J, Zhang XE, Deng J, Ge F**. 2014. Acetylome analysis reveals diverse functions of lysine acetylation in *Mycobacterium tuberculosis*. Mol Cell Proteomics **13:**3352–3360. http://dx.doi.org/10.1074/mcp.M114.041962.

40. **Liao G, Xie L, Li X, Cheng Z, Xie J**. 2014. Unexpected extensive lysine acetylation in the trump-card antibiotic producer *Streptomyces roseosporus* revealed by proteome-wide profiling. J Proteomics **106:**260–269. http://dx.doi.org/10.1016/j.jprot.2014.04.017.

41. **Xie L, Wang X, Zeng J, Zhou M, Duan X, Li Q, Zhang Z, Luo H, Pang L, Li W, Liao G, Yu X, Li Y, Huang H, Xie J**. 2015. Proteome-wide lysine acetylation profiling of the human pathogen *Mycobacterium tuberculosis*. Int J Biochem Cell Biol **59:**193–202. http://dx.doi.org/10.1016/j.biocel.2014.11.010.

42. **van Noort V, Seebacher J, Bader S, Mohammed S, Vonkova I, Betts MJ, Kühner S, Kumar R, Maier T, O'Flaherty M, Rybin V, Schmeisky A, Yus E, Stülke J, Serrano L, Russell RB, Heck AJ, Bork P, Gavin AC**. 2012. Cross-talk between phosphorylation and lysine acetylation in a genome-reduced bacterium. Mol Syst Biol **8:**571. http://dx.doi.org/10.1038/msb.2012.4.

43. **Kosono S, Tamura M, Suzuki S, Kawamura Y, Yoshida A, Nishiyama M, Yoshida M**. 2015. Changes in the acetylome and succinylome of *Bacillus subtilis* in response to carbon source. PLoS One **10:**e0131169. http://dx.doi.org/10.1371/journal.pone.0131169.

44. **Starai VJ, Gardner JG, Escalante-Semerena JC**. 2005. Residue Leu-641 of acetyl-CoA synthetase is critical for the acetylation of residue Lys-609 by the protein acetyltransferase enzyme of *Salmonella enterica*. J Biol Chem **280:**26200–26205. http://dx.doi.org/10.1074/jbc.M504863200.

45. **Gardner JG, Grundy FJ, Henkin TM, Escalante-Semerena JC**. 2006. Control of acetyl-coenzyme A synthetase (AcsA) activity by acetylation/deacetylation without NAD(+) involvement in *Bacillus subtilis*. J Bacteriol **188:**5460–5468. http://dx.doi.org/10.1128/JB.00215-06.

46. **Schwer B, Bunkenborg J, Verdin RO, Andersen JS, Verdin E**. 2006. Reversible lysine acetylation controls the activity of the mitochondrial enzyme acetyl-CoA synthetase 2. Proc Natl Acad Sci U S A **103:**10224–10229. http://dx.doi.org/10.1073/pnas.0603968103.

47. **Tucker AC, Escalante-Semerena JC**. 2013. Acetoacetyl-CoA synthetase activity is controlled by a protein acetyltransferase with unique domain organization in *Streptomyces lividans*. Mol Microbiol **87:**152–167. http://dx.doi.org/10.1111/mmi.12088.

48. **Mikulik K, Felsberg J, Kudrnáčová E, Bezoušková S, Setinová D, Stodůlková E, Zídková J, Zídek V**. 2012. CobB1 deacetylase activity in *Streptomyces coelicolor*. Biochem Cell Biol **90:**179–187. http://dx.doi.org/10.1139/o11-086.

49. **Hayden JD, Brown LR, Gunawardena HP, Perkowski EF, Chen X, Braunstein M**. 2013. Reversible acetylation regulates acetate and propionate metabolism in *Mycobacterium smegmatis*. Microbiology **159:**1986–1999. http://dx.doi.org/10.1099/mic.0.068585-0.

50. **Xu H, Hegde SS, Blanchard JS**. 2011. Reversible acetylation and inactivation of *Mycobacterium tuberculosis* acetyl-CoA synthetase is dependent on cAMP. Biochemistry **50:**5883–5892. http://dx.doi.org/10.1021/bi200156t.

51. **Gardner JG, Escalante-Semerena JC**. 2008. Biochemical and mutational analyses of AcuA, the acetyltransferase enzyme that controls the activity of the acetyl coenzyme A synthetase (AcsA) in *Bacillus subtilis*. J Bacteriol **190:**5132–5136. http://dx.doi.org/10.1128/JB.00340-08.

52. **Gardner JG, Escalante-Semerena JC**. 2009. In Bacillus subtilis, the sirtuin protein deacetylase, encoded by the srtN gene (formerly yhdZ), and functions encoded by the acuABC genes control the activity of acetyl coenzyme A synthetase. J Bacteriol **191:**1749–1755. http://dx.doi.org/10.1128/JB.01674-08.

53. **Mi H, Muruganujan A, Casagrande JT, Thomas PD**. 2013. Large-scale gene function analysis with the PANTHER classification system. Nat Protoc **8:**1551–1566. http://dx.doi.org/10.1038/nprot.2013.092.

54. **Muntel J, Fromion V, Goelzer A, Maabeta S, Mäder U, Büttner K, Hecker M, Becher D**. 2014. Comprehensive absolute quantification of the cytosolic proteome of *Bacillus subtilis* by data independent, parallel fragmentation in liquid chromatography/mass spectrometry (LC/MS(E)). Mol Cell Proteomics **13:**1008–1019. http://dx.doi.org/10.1074/mcp.M113.032631.

55. **Dubnau D**. 1991. Genetic competence in *Bacillus subtilis*. Microbiol Rev **55:**395–424.

56. **Baeza J, Dowell JA, Smallegan MJ, Fan J, Amador-Noguez D, Khan Z, Denu JM**. 2014. Stoichiometry of site-specific lysine acetylation in an entire proteome. J Biol Chem **289:**21326–21338. http://dx.doi.org/10.1074/jbc.M114.581843.

57. **Zencheck WD, Xiao H, Weiss LM**. 2012. Lysine post-translational modifications and the cytoskeleton. Essays Biochem **52:**135–145. http://dx.doi.org/10.1042/bse0520135.

58. **Sadoul K, Wang J, Diagouraga B, Khochbin S**. 2011. The tale of protein lysine acetylation in the cytoplasm. J Biomed Biotechnol **2011:**970382. http://dx.doi.org/10.1155/2011/970382.

59. **Jones LJ, Carballido-López R, Errington J**. 2001. Control of cell shape in bacteria: helical, actin-like filaments in *Bacillus subtilis*. Cell **104:**913–922. http://dx.doi.org/10.1016/S0092-8674(01)00287-2.

60. **Formstone A, Errington J**. 2005. A magnesium-dependent *mreB* null mutant: implications for the role of *mreB* in *Bacillus subtilis*. Mol Microbiol **55:**1646–1657. http://dx.doi.org/10.1111/j.1365-2958.2005.04506.x.

61. **Domínguez-Escobar J, Chastanet A, Crevenna AH, Fromion V, Wedlich-Söldner R, Carballido-López R**. 2011. Processive movement of MreB-associated cell wall biosynthetic complexes in bacteria. Science **333:**225–228. http://dx.doi.org/10.1126/science.1203466.

62. **Garner EC, Bernard R, Wang W, Zhuang X, Rudner DZ, Mitchison T**. 2011. Coupled, circumferential motions of the cell wall synthesis machinery and MreB filaments in *B. subtilis*. Science **333:**222–225. http://dx.doi.org/10.1126/science.1203285.

63. **Strahl H, Burmann F, Hamoen LW**. 2014. The actin homologue MreB organizes the bacterial cell membrane. Nat Commun **5:**3442. http://dx.doi.org/10.1038/ncomms4442.

64. **Kamieniarz K, Schneider R**. 2009. Tools to tackle protein acetylation. Chem Biol **16:**1027–1029. http://dx.doi.org/10.1016/j.chembiol.2009.10.002.

65. **Kawai Y, Asai K, Errington J**. 2009. Partial functional redundancy of MreB isoforms, MreB, Mbl and MreBH, in cell morphogenesis of *Bacillus subtilis*. Mol Microbiol **73:**719–731. http://dx.doi.org/10.1111/j.1365-2958.2009.06805.x.

66. **Svinkina T, Gu H, Silva JC, Mertins P, Qiao J, Fereshetian S, Jaffe JD, Kuhn E, Udeshi ND, Carr SA**. 2015. Deep, quantitative coverage of the lysine acetylome using novel anti-acetyl-lysine antibodies and an optimized proteomic workflow. Mol Cell Proteomics **14:**2429–2440. http://dx.doi.org/10.1074/mcp.O114.047555.

67. **Lundby A, Lage K, Weinert BT, Bekker-Jensen DB, Secher A, Skovgaard T, Kelstrup CD, Dmytriyev A, Choudhary C, Lundby C, Olsen JV**. 2012. Proteomic analysis of lysine acetylation sites in rat tissues reveals organ specificity and subcellular patterns. Cell Rep **2:**419–431. http://dx.doi.org/10.1016/j.celrep.2012.07.006.

68. **Jeffers V, Sullivan WJ, Jr.** 2012. Lysine acetylation is widespread on proteins of diverse function and localization in the protozoan parasite *Toxoplasma gondii*. Eukaryot Cell **11:**735–742. http://dx.doi.org/10.1128/EC.00088-12.

69. **Shao J, Xu D, Hu L, Kwan YW, Wang Y, Kong X, Ngai SM**. 2012. Systematic analysis of human lysine acetylation proteins and accurate prediction of human lysine acetylation through bi-relative adapted binomial score Bayes feature representation. Mol Biosyst **8:**2964–2973. http://dx.doi.org/10.1039/c2mb25251a.

70. **Miao J, Lawrence M, Jeffers V, Zhao F, Parker D, Ge Y, Sullivan WJ,**

Jr, Cui L. 2013. Extensive lysine acetylation occurs in evolutionarily conserved metabolic pathways and parasite-specific functions during *Plasmodium falciparum* intraerythrocytic development. Mol Microbiol **89:**660–675. http://dx.doi.org/10.1111/mmi.12303.

71. **Berndsen CE, Denu JM**. 2008. Catalysis and substrate selection by histone/protein lysine acetyltransferases. Curr Opin Struct Biol **18:**682–689. http://dx.doi.org/10.1016/j.sbi.2008.11.004.

72. **Crosby HA, Escalante-Semerena JC**. 2014. The acetylation motif in AMP-forming acyl coenzyme A synthetases contains residues critical for acetylation and recognition by the protein acetyltransferase Pat of *Rhodopseudomonas palustris*. J Bacteriol **196:**1496–1504. http://dx.doi.org/10.1128/JB.00004-14.

73. **Wagner GR, Payne RM**. 2013. Widespread and enzyme-independent N-epsilon-acetylation and N-epsilon-succinylation of proteins in the chemical conditions of the mitochondrial matrix. J Biol Chem **288:**29036–29045. http://dx.doi.org/10.1074/jbc.M113.486753.

74. **Baeza J, Smallegan MJ, Denu JM**. 2015. Site-specific reactivity of nonenzymatic lysine acetylation. ACS Chem Biol **10:**122–128. http://dx.doi.org/10.1021/cb500848p.

75. **Tanner KG, Trievel RC, Kuo MH, Howard RM, Berger SL, Allis CD, Marmorstein R, Denu JM**. 1999. Catalytic mechanism and function of invariant glutamic acid 173 from the histone acetyltransferase GCN5 transcriptional coactivator. J Biol Chem **274:**18157–18160. http://dx.doi.org/10.1074/jbc.274.26.18157.

76. **Trievel RC, Rojas JR, Sterner DE, Venkataramani RN, Wang L, Zhou J, Allis CD, Berger SL, Marmorstein R**. 1999. Crystal structure and mechanism of histone acetylation of the yeast GCN5 transcriptional coactivator. Proc Natl Acad Sci U S A **96:**8931–8936. http://dx.doi.org/10.1073/pnas.96.16.8931.

77. **Liszczak G, Arnesen T, Marmorstein R**. 2011. Structure of a ternary Naa50p (NAT5/SAN) N-terminal acetyltransferase complex reveals the molecular basis for substrate-specific acetylation. J Biol Chem **286:**37002–37010. http://dx.doi.org/10.1074/jbc.M111.282863.

78. **Shioi JI, Matsuura S, Imae Y**. 1980. Quantitative measurements of proton motive force and motility in *Bacillus subtilis*. J Bacteriol **144:**891–897.

79. **van den Ent F, Izoré T, Bharat TA, Johnson CM, Löwe J**. 2014. Bacterial actin MreB forms antiparallel double filaments. eLife **3:**e02634. http://dx.doi.org/10.7554/eLife.02634.

80. **Schirner K, Eun YJ, Dion M, Luo Y, Helmann JD, Garner EC, Walker S**. 2015. Lipid-linked cell wall precursors regulate membrane association of bacterial actin MreB. Nat Chem Biol **11:**38–45. http://dx.doi.org/10.1038/nchembio.1689.

81. **Kawai Y, Daniel RA, Errington J**. 2009. Regulation of cell wall morphogenesis in *Bacillus subtilis* by recruitment of PBP1 to the MreB helix. Mol Microbiol **71:**1131–1144. http://dx.doi.org/10.1111/j.1365-2958.2009.06601.x.

82. **Favini-Stabile S, Contreras-Martel C, Thielens N, Dessen A**. 2013. MreB and MurG as scaffolds for the cytoplasmic steps of peptidoglycan biosynthesis. Environ Microbiol **15:**3218–3228. http://dx.doi.org/10.1111/1462-2920.12171.

83. **Muchová K, Chromiková Z, Barák I**. 2013. Control of *Bacillus subtilis* cell shape by RodZ. Environ Microbiol **15:**3259–3271. http://dx.doi.org/10.1111/1462-2920.12200.

84. **Rueff AS, Chastanet A, Domínguez-Escobar J, Yao Z, Yates J, Prejean MV, Delumeau O, Noirot P, Wedlich-Söldner R, Filipe SR, Carballido-López R**. 2014. An early cytoplasmic step of peptidoglycan synthesis is associated with MreB in *Bacillus subtilis*. Mol Microbiol **91:**348–362. http://dx.doi.org/10.1111/mmi.12467.

85. **Ganchev DN, Hasper HE, Breukink E, de Kruijff B**. 2006. Size and orientation of the lipid II headgroup as revealed by AFM imaging. Biochemistry **45:**6195–6202. http://dx.doi.org/10.1021/bi051913e.

86. **Wang X, Hayes JJ**. 2008. Acetylation mimics within individual core histone tail domains indicate distinct roles in regulating the stability of higher-order chromatin structure. Mol Cell Biol **28:**227–236. http://dx.doi.org/10.1128/MCB.01245-07.

87. **Simonsson M, Kanduri M, Grönroos E, Heldin CH, Ericsson J**. 2006. The DNA binding activities of Smad2 and Smad3 are regulated by coactivator-mediated acetylation. J Biol Chem **281:**39870–39880. http://dx.doi.org/10.1074/jbc.M607868200.

88. **Hecht A, Laroche T, Strahl-Bolsinger S, Gasser SM, Grunstein M**. 1995. Histone H3 and H4 N-termini interact with SIR3 and SIR4 proteins: a molecular model for the formation of heterochromatin in yeast. Cell **80:**583–592. http://dx.doi.org/10.1016/0092-8674(95)90512-X.

89. **Yang Y, Rao R, Shen J, Tang Y, Fiskus W, Nechtman J, Atadja P, Bhalla K**. 2008. Role of acetylation and extracellular location of heat shock protein 90 alpha in tumor cell invasion. Cancer Res **68:**4833–4842. http://dx.doi.org/10.1158/0008-5472.CAN-08-0644.

90. **Li M, Luo J, Brooks CL, Gu W**. 2002. Acetylation of p53 inhibits its ubiquitination by Mdm2. J Biol Chem **277:**50607–50611. http://dx.doi.org/10.1074/jbc.C200578200.

91. **Kawai Y, Garduño L, Theodore M, Yang J, Arinze IJ**. 2011. Acetylation-deacetylation of the transcription factor Nrf2 (nuclear factor erythroid 2-related factor 2) regulates its transcriptional activity and nucleocytoplasmic localization. J Biol Chem **286:**7629–7640. http://dx.doi.org/10.1074/jbc.M110.208173.

92. **Sun Y, Xu Y, Roy K, Price BD**. 2007. DNA damage-induced acetylation of lysine 3016 of ATM activates ATM kinase activity. Mol Cell Biol **27:**8502–8509. http://dx.doi.org/10.1128/MCB.01382-07.

93. **Albano M, Hahn J, Dubnau D**. 1987. Expression of competence genes in *Bacillus subtilis*. J Bacteriol **169:**3110–3117.

94. **Mukherjee S, Babitzke P, Kearns DB**. 2013. FliW and FliS function independently to control cytoplasmic flagellin levels in *Bacillus subtilis*. J Bacteriol **195:**297–306. http://dx.doi.org/10.1128/JB.01654-12.

95. **Carabetta VJ, Silhavy TJ, Cristea IM**. 2010. The response regulator SprE (RssB) is required for maintaining poly(A) polymerase I-degradosome association during stationary phase. J Bacteriol **192:**3713–3721. http://dx.doi.org/10.1128/JB.00300-10.

96. **Cristea IM, Williams R, Chait BT, Rout MP**. 2005. Fluorescent proteins as proteomic probes. Mol Cell Proteomics **4:**1933–1941. http://dx.doi.org/10.1074/mcp.M500227-MCP200.

97. **Carabetta VJ, Tanner AW, Greco TM, Defrancesco M, Cristea IM, Dubnau D**. 2013. A complex of YlbF, YmcA and YaaT regulates sporulation, competence and biofilm formation by accelerating the phosphorylation of Spo0A. Mol Microbiol **88:**283–300. http://dx.doi.org/10.1111/mmi.12186.

98. **Guan KL, Yu W, Lin Y, Xiong Y, Zhao S**. 2010. Generation of acetyllysine antibodies and affinity enrichment of acetylated peptides. Nat Protoc **5:**1583–1595. http://dx.doi.org/10.1038/nprot.2010.117.

99. **Kulak NA, Pichler G, Paron I, Nagaraj N, Mann M**. 2014. Minimal, encapsulated proteomic-sample processing applied to copy-number estimation in eukaryotic cells. Nat Methods **11:**319–324. http://dx.doi.org/10.1038/nmeth.2834.

100. **Cox J, Hein MY, Luber CA, Paron I, Nagaraj N, Mann M**. 2014. Accurate proteome-wide label-free quantification by delayed normalization and maximal peptide ratio extraction, termed MaxLFQ. Mol Cell Proteomics **13:**2513–2526. http://dx.doi.org/10.1074/mcp.M113.031591.

101. **Wiśniewski JR, Hein MY, Cox J, Mann M**. 2014. A "proteomic ruler" for protein copy number and concentration estimation without spike-in standards. Mol Cell Proteomics **13:**3497–3506. http://dx.doi.org/10.1074/mcp.M113.037309.

102. **Bindea G, Mlecnik B, Hackl H, Charoentong P, Tosolini M, Kirilovsky A, Fridman WH, Pagès F, Trajanoski Z, Galon J**. 2009. ClueGO: a cytoscape plug-in to decipher functionally grouped Gene Ontology and pathway annotation networks. Bioinformatics **25:**1091–1093. http://dx.doi.org/10.1093/bioinformatics/btp101.

103. **Szklarczyk D, Franceschini A, Wyder S, Forslund K, Heller D, Huerta-Cepas J, Simonovic M, Roth A, Santos A, Tsafou KP, Kuhn M, Bork P, Jensen LJ, von Mering C**. 2015. STRING v10: protein-protein interaction networks, integrated over the tree of life. Nucleic Acids Res **43:**D447–D452. http://dx.doi.org/10.1093/nar/gku1003.

104. **Shannon P, Markiel A, Ozier O, Baliga NS, Wang JT, Ramage D, Amin N, Schwikowski B, Ideker T**. 2003. Cytoscape: a software environment for integrated models of biomolecular interaction networks. Genome Res **13:**2498–2504. http://dx.doi.org/10.1101/gr.1239303.

105. **Hornbeck PV, Kornhauser JM, Tkachev S, Zhang B, Skrzypek E, Murray B, Latham V, Sullivan M**. 2012. PhosphoSitePlus: a comprehensive resource for investigating the structure and function of experimentally determined post-translational modifications in man and mouse. Nucleic Acids Res **40:**D261–D270. http://dx.doi.org/10.1093/nar/gkr1122.

106. **Guex N, Peitsch MC**. 1997. SWISS-MODEL and the Swiss-PdbViewer: an environment for comparative protein modeling. Electrophoresis **18:**2714–2723. http://dx.doi.org/10.1002/elps.1150181505.

107. **Larkin MA, Blackshields G, Brown NP, Chenna R, McGettigan PA, McWilliam H, Valentin F, Wallace IM, Wilm A, Lopez R, Thompson JD, Gibson TJ, Higgins DG**. 2007. Clustal W and Clustal X version 2.0.

Bioinformatics **23:**2947–2948. http://dx.doi.org/10.1093/bioinformatics/btm404.

108. **Pagano M, Gauvreau K**. 2000. Principles of biostatistics, 2nd ed. Duxbury Thomson Learning, Pacific Grove, CA.

109. **Sedgwick P**. 2014. Spearman's rank correlation coefficient. BMJ **349:** g7327. http://dx.doi.org/10.1136/bmj.g7327.

110. **Guan KL, Xiong Y**. 2011. Regulation of intermediary metabolism by protein acetylation. Trends Biochem Sci **36:**108–116. http://dx.doi.org/10.1016/j.tibs.2010.09.003.

111. **Anderson KA, Hirschey MD**. 2012. Mitochondrial protein acetylation regulates metabolism. Essays Biochem **52:**23–35. http://dx.doi.org/10.1042/bse0520023.

112. **König AC, Hartl M, Boersema PJ, Mann M, Finkemeier I**. 2014. The mitochondrial lysine acetylome of *Arabidopsis*. Mitochondrion **19:** 252–260. http://dx.doi.org/10.1016/j.mito.2014.03.004.

113. **Turgay K, Hahn J, Burghoorn J, Dubnau D**. 1998. Competence in *Bacillus subtilis* is controlled by regulated proteolysis of a transcription factor. EMBO J **17:**6730–6738. http://dx.doi.org/10.1093/emboj/17.22.6730.